COMPARISON OF DONOR-ACCEPTOR-DONOR TYPE CONJUGATED SYSTEMS WITH CROSS-EXCHANGE OF DONOR UNITS

A THESIS SUBMITTED TO
THE GRADUATE SCHOOL OF NATURAL AND APPLIED SCIENCES
OF
MIDDLE EAST TECHNICAL UNIVERSITY

BY

DENİZ EROĞLU

IN PARTIAL FULFILLMENT OF THE REQUIREMENTS
FOR
THE DEGREE OF MASTER OF SCIENCE
IN
CHEMISTRY

NOVEMBER 2020

Approval of the thesis:

COMPARISON OF DONOR-ACCEPTOR-DONOR TYPE CONJUGATED SYSTEMS WITH CROSS-EXCHANGE OF DONOR UNITS

submitted by **DENİZ EROĞLU** in partial fulfillment of the requirements for the degree of **Master of Science** i**n Chemistry, Middle East Technical University** by,

Prof. Dr. Halil Kalıpçılar
Dean, Graduate School of **Natural and Applied Sciences** _____

Prof. Dr. Cihangir Tanyeli
Head of the Department, **Chemistry** _____

Prof. Dr. Ahmet M. Önal
Supervisor, **Chemistry, METU** _____

Assoc. Prof. Dr. Emine Gül Cansu Ergün
Co-Supervisor, **Electrical and Electronics Eng., Başkent University** _____

Examining Committee Members:

Prof. Dr. Ali Çırpan
Chemistry, METU _____

Prof. Dr. Ahmet M. Önal
Chemistry, METU _____

Assoc. Prof. Dr. Emine Gül Cansu Ergün
Electrical and Electronics Eng., Başkent University _____

Assoc. Prof. Dr. Akın Akdağ
Chemistry, METU _____

Assist. Prof. Dr. Demet Asil Alptekin
Chemistry, METU _____

Date: 23.11.2020

I hereby declare that all information in this document has been obtained and presented in accordance with academic rules and ethical conduct. I also declare that, as required by these rules and conduct, I have fully cited and referenced all material and results that are not original to this work.

Name Last name : Deniz Eroğlu

Signature :

ABSTRACT

COMPARISON OF DONOR-ACCEPTOR-DONOR TYPE CONJUGATED SYSTEMS WITH CROSS-EXCHANGE OF DONOR UNITS

Eroğlu, Deniz
Master of Science, Chemistry
Supervisor : Prof. Dr. Ahmet M. Önal
Co-Supervisor: Assoc. Prof. Dr. Emine Gül Cansu Ergün

November 2020, 56 pages

In this thesis study, a series of new donor-acceptor donor type monomers were synthesized. For this purpose, benzothiadiazole (B) was used as the acceptor unit. Donor units, carbazole (C) and thiophene (T), were combined to B unit both symmetrically (**CBC** and **CTBTC**) and unsymmetrically (**CBT**) to understand the effect of cross exchange of donor units on the opto-electronic properties of monomers. The monomers were characterized using Nuclear Magnetic Resonance (NMR) and High-Resolution Mass (HRMS) spectroscopies. Optical properties of monomers were investigated by using UV-visible and fluorescence spectroscopy. Replacing one of the symmetrical carbazole units in **CBC** monomer with thiophene unit results in about 8 nm red shift in optical absorption. Having both carbazole and thiophene units symmetrically in the monomer structure increases the conjugation and exhibits about 70 nm red shift in the optical absorption. On the other, electrochemical behaviour of monomers were investigated utilizing cyclic and differential pulse voltammetry techniques. As a result of these studies, **CTBTC** monomer was found to have the lowest oxidation potential and it has the lowest band gap energy (both optical and electronic) due to increased conjugation. After their characterization, monomers were polymerized electrochemically and properties of

polymers were also investigated to understand the effect of symmetrical (D-A-D type) and unsymmetrical (D-A-D' type) combination of donor units. Polymerization of **CBT** and **CTBTC** monomers was successfully achieved, and P**CTBTC** shows multichromic behavior however, its stability was lower than the stability of P**CBT**. The percent transmittance value of P**CBT** was measured as 12% at 530 nm and the switching time was calculated as 3 s at 95% of the full contrast. For P**CTBTC**, on the other hand, at 576 nm, percent transmittance and the switching time was found as 8% and 4.2 s, respectively. It was observed that P**CTBTC** has the lowest optical band gap value and this value was calculated as 1.44 eV. For P**CBT**, the optical band gap was calculated as 1.81 eV.

Keywords: Carbazole, thiophene, benzothiadiazole, donor-acceptor-donor, electrochromic polymers

ÖZ

VERİCİ-ALICI-VERİCİ TİPİ KONJUGE SİSTEMLERİN VERİCİ BİRİMLERİNİN ÇAPRAZ DEĞİŞİMİ İLE KARŞILAŞTIRILMASI

Eroğlu, Deniz
Yüksek Lisans, Kimya
Tez Yöneticisi: Prof. Dr. Ahmet M. Önal
Ortak Tez Yöneticisi: Doç. Dr. Emine Gül Cansu Ergün

Kasım 2020, 56 sayfa

Bu tez çalışmasında, bir dizi yeni verici-alıcı-verici tipi monomer sentezlenmiştir. Bu amaçla, alıcı birim olarak benzotiadiazol (B) kullanılmış ve verici birimlerin çapraz değişiminin monomerlerin opto-elektronik özellikleri üzerindeki etkisini anlamak için karbazol (C) ve tiyofen (T) üniteleri B ünitesiyle hem simetrik (**CBC** ve **CTBTC**) hem de asimetrik (**CBT**) şekilde birleştirilmiştir. Sentezlenen monomerler Nükleer Manyetik Rezonans (NMR) ve Yüksek Çözünürlüklü Kütle (HRMS) spektroskopisi kullanılarak karakterize edilmiştir. Monomerlerin optik özellikleri UV-görünür ve floresan spektroskopisi kullanılarak, elektrokimyasal davranışları ise Döngüsel ve Diferansiyel Darbe Voltametrisi kullanılarak incelenmiştir. **CBC** monomerindeki simetrik karbazol birimlerinden birinin tiyofen birimi ile değiştirilmesi, optik absorpsiyonda yaklaşık 8 nm kırmızı kayma ile sonuçlanmıştır. Monomer yapısında simetrik olarak hem karbazol hem de tiyofen birimlerine sahip olmak, konjugasyonu arttırmış ve optik absorpsiyonda yaklaşık 70 nm kırmızı kayma gözlemlenmesine sebep olmuştur. Karakterizasyonlarından sonra, monomerler elektrokimyasal olarak polimerleştirilmiş ve verici birimlerinin simetrik (D-A-D tipi) ve simetrik olmayan (D-A-D' tipi) kombinasyonunun etkisini

araştırmak için elde edilen polimerlerin optik ve elektrokimyasal özellikleri de incelenmiştir. **CBT** ve **CTBTC** monomerlerinin polimerizasyonu başarıyla gerçekleştirilmiş ve P**CTBTC**'nin multikromik davranış göstertiği gözlemlenmiştir, ancak stabilitesi P**CBT**'nin stabilitesinden daha düşük olarak bulunmuştur. P**CBT**'nin yüzde geçirgenlik değeri 530 nm'de %12 olarak ölçülmüş ve tam kontrastın % 95'inde anahtarlama süresi 3 saniye olarak hesaplanmıştır. P**CTBTC** için ise 576 nm'de geçirgenlik yüzdesi ve anahtarlama süresi sırasıyla %8 ve 4,2 sn olarak bulunmuştur. P**CTBTC**'nin en düşük optik bant aralığı değerine sahip olduğu gözlemlenmiş ve bu değer 1.44 eV olarak hesaplanmıştır. P**CBT** için ise optik bant aralığı 1.81 eV olarak hesaplanmıştır.

Anahtar Kelimeler: Karbazol, tiyofen, benzotiadiazol, verici-alıcı-verici, elektrokromik polimerler

To my family…

ACKNOWLEDGMENTS

I would like to express my sincere gratitude to Prof. Dr. Ahmet M. Önal for giving me the opportunity to study in his laboratory. Also, I would like to thank him for giving me to chance to make experiments together and the opportunity to benefit from his experiences. His endless care and support for his students made me feel not alone. I will always be honored since I will be graduated as his student.

I would like to thank my co-advisor Assoc. Prof. Dr. Emine Gül Cansu Ergün for her guidance, infinite support, important advices, and endless motivation about my thesis study.

I would like to thank Assoc. Prof. Dr. Akın Akdağ for his support and help since the beginning of my university life.

I would like to thank Yeter Eroğlu, Ahmet Eroğlu, Nurşen Eroğlu and Mahmut Fındık Mamasıyanık for their support and love.

I would like to thank my laboratory mates Deniz Çakal, Yalçın Boztaş, Elif Demir Arabacı, Merve Akbayrak and Samet Şanlı for their friendship.

I would like to thank my dear friends Oğuzhan Albayrak, Merve Yıldırım, Hakan Özcan, Çiğdem Acar, Üstün Utkan Acar, Deniz Keskin and Dilara Gençtürk for their friendship, love and support. Even though we can't be together I know they are always with me.

TABLE OF CONTENTS

LIST OF TABLES

TABLES

LIST OF FIGURES

FIGURES

LIST OF SCHEMES

SCHEMES

LIST OF ABBREVIATIONS

ABBREVIATIONS

A	Acceptor
ACN	Acetonitrile
B	Benzothiadiazole
C	9-Benzyl-9*H*-carbazole
CB	Conduction Band
CBC	4,7-bis(9-benzyl-9H-carbazol-3-yl)benzo[c][1,2,5]thiadiazole
CBT	4-(9-benzyl-9H-carbazol-3-yl)-7-(thiophen-2-yl)benzo[c][1,2,5]thiadiazole
CE	Counter Electrode
CP	Conducting Polymers
CTBTC	4,7-bis(5-(9-benzyl-9H-carbazol-3-yl)thiophen-2-yl)benzo[c][1,2,5] thiadiazole
CV	Cyclic Voltammetry
D	Donor
D-A-D	Donor-Acceptor-Donor
DCM	Dichloromethane
DMSO	Dimethylsulfoxide
DPP	Diketopyrrolopyrrole
DPV	Differential Pulse Voltammetry

ECD	Electrochromic Device
E_g	Bandgap Energy
E^{ox}	Oxidation potential
E^{red}	Reduction potential
FET	Field Effect Transistor
GOx	Glucose oxidase
GRIM	Grignard Metathesis
HOMO	Highest Ocuupied Molecular Orbital
HRMS	High Resolution Mass Spectroscopy
ICT	Intramolecular Charge Transfer
ITO	Indium tin oxide
LUMO	Lowest Unoccupied Molecular Orbital
NMR	Nuclear Magnetic Resonance
OLED	Organic Light Emitting Diode
ε	Dielectric Constant

CHAPTER 1

INTRODUCTION

1.1 Conjugated (Conducting) Polymers

Polymeric materials have been used by humanity for hundreds of years because of their several advantages. Natural polymers such as wool, silk, cellulose have been chosen as clothing or thermally insulating materials. Synthetic polymers, on the other hand, have applications in wider areas of life with respect to natural polymers. Today, they are used in different areas of life, especially in most common consumer goods.

Polymers were known to be electrically insulating material until 1977, and they were used as insulators in the electric sector. However, three scientists: Hideki Shirakawa, Alan Heeger, and Alan MacDiarmid discovered that polymers could be electrically conductive via doping process, and they received Nobel Prize in 2000 [1]. Polyacetylene film was prepared from acetylene by using Ziegler-Natta catalyst. When the film was exposed to halogen vapor, i.e., iodine, it is observed that its conductivity increased by more than 10^7 times [2]. This discovery paved the way for the use of polymers in many different areas and in a more convenient way. Their characteristic conductivity comes from conjugated π-electrons on the backbone chain[3], and they respond to electric and magnetic fields easily. Because of their high and tunable conductivity, conducting polymers are good candidates for several optoelectronic applications, for instance, electrochromic devices (ECDs) [4], smart windows [5], displays [6], organic light emitting diodes (OLEDs) [7], organic solar cells (OSCs) [8], biosensors [9] and camouflage materials [10]. Examples of some common conducting polymers are shown in Figure 1.1.

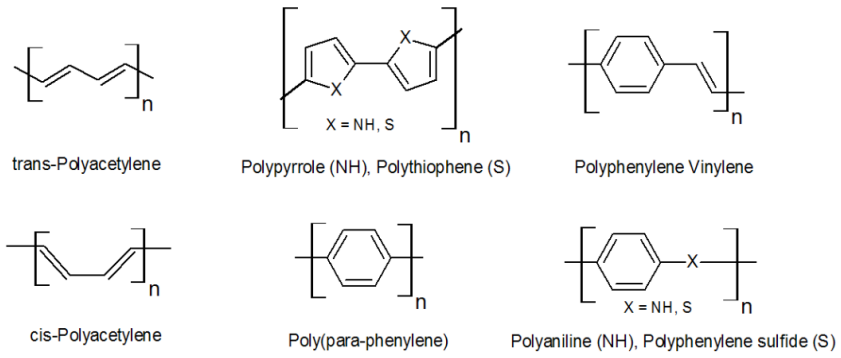

Figure 1.1.Some common conjugated polymers.

The discovery of the capability of some polymers to be electrically conductive made a significant impact in the scientific world. For over 50 years, the countless number of discoveries have been made in this field. In Figure 1.2, milestones in conjugated conducting polymer field are shown. Usage of conducting polymers in biosensors, photovoltaic cells, transistors, electrochromic devices and supercapacitors can be accepted as the revolutionary turning points for not only scientific curiosity but also industry.

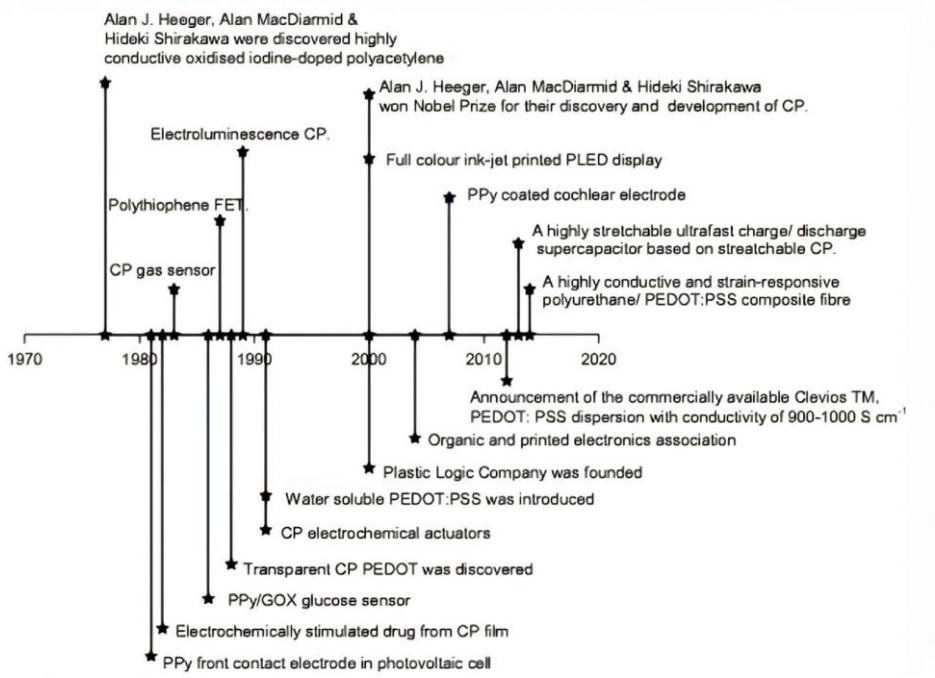

Figure 1.2. Milestones in conjugated polymers [11].

Conjugated polymeric materials with an aromatic backbone are much more preferred due to their significant number of advantages over conjugated polymeric materials with an aliphatic backbone. The most significant advantage of having an aromatic backbone for a conductive polymer is its stability. Because scientists and manufacturers have had several problems with polyacetylene, like its poor stability and poor processability, they have started studying with conjugated polymers that have an aromatic backbone [12]. Observation of having improved stability of aromatic conjugated polymers leads to further studies conducted with this type of materials in the literature. Polyheterocycles, especially conjugated five-membered electron-rich rings, are highly flexible. Thiophenes, selenophenes, furans, and pyrroles are the common examples of these systems and the heteroatom on the ring affects the oxidation potential and bandgap of the polymer [13].

The main advantage of synthetic conjugated polymers is that their characteristics can be tuned through synthetic methods. Electrochromic properties of the conjugated polymers can be altered by utilizing the synthetic methods of the material. Substitutions (especially 3,4-substitutions), bridging alkyl units (ethylene,

propylene, methylenedioxy, etc.) and N-functionalization of electron-rich pyrrole heterocycles are frequently preferred synthetic methods in the literature [14].

1.2 The Conductivity and Conductivity Mechanism of Conjugated Polymers

Conjugated polymers are usually classified as semiconductors with having a conductivity range of 10^{-10} to 10^{4} S/cm [3]. According to usage area of the polymer, their conductivity can be tuned by changing the several properties of the polymer, mainly the bandgap. The application area usually determines the desired conductivity of the polymer. For example, low bandgap polymers are very suitable for solar cell applications [14].

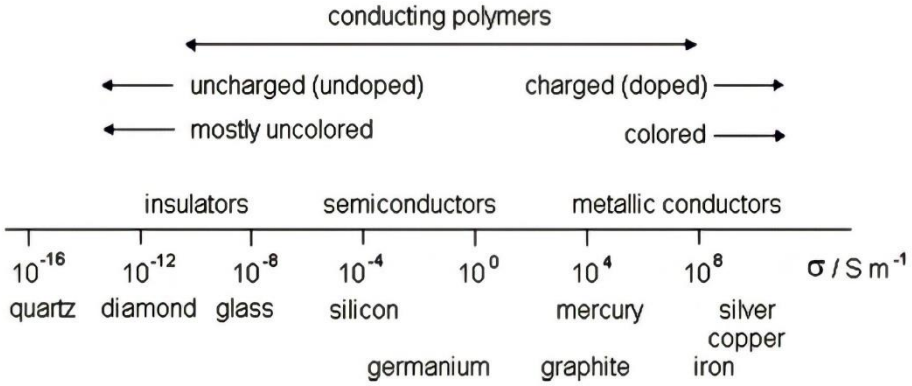

Figure 1.3. Electrical conductivity range of conducting polymers

The electrical conductivity range of conjugated polymers is shown in Figure 1.3. and it can be concluded that scientists can mimic most of the commonly used semiconducting materials in terms of electrical conductivity by obtaining a conductive polymer with the same electronic properties. Doping increases the mobility of the charge through the backbone of the polymer and hence conductivity [12].

1.2.1 Band Gap

The valence band is formed by the highest occupied molecular orbital (HOMO) and the conduction band is provided by lowest unoccupied molecular orbital (LUMO), in scientific terminology. E_g i.e. the band gap energy comprises an electronic transition from the top of the valence band to the bottom of the conduction band. As shown in Figure 1.4. substances with large band gaps ($Eg \geq 3.0$ eV [4]) are insulators, those with smaller band gaps are semiconductors.

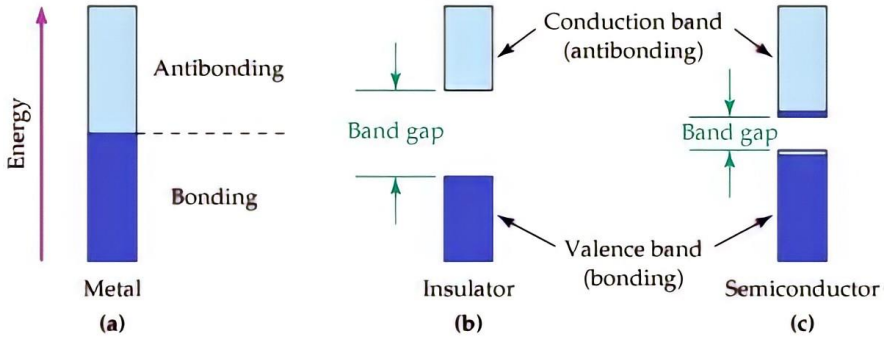

Figure 1.4. Energy bands in solids

In general, conjugated polymers exhibit very low conductivities unless they are p-doped via oxidation or n-doped via reduction. Doping process can be either achieved chemically or electrochemically. A dopant is used in its vapor or solution form in the reaction mixture during the doping process in chemical methods. However, in electrochemical methods, the monomer (during polymer electrosynthesis) or the polymer and dopant are dissolved in a proper solvent that has a suitable potential window and solubility [3].

The conductivity of undoped conjugated polymers can be increased up to 10^{12} by doping process [12]. Charge carriers, polarons and bipolarons, are introduced within the polymer chain during the doping process as shown in Figure 1.5. Their movement through the polymer backbone results in an electric current. Smaller bandgap obtained by doping provides higher conductivity [15].

During an oxidation process of a conjugated polymer, electrons are removed from the system and this results in the creation of holes (radical cation or polaron). Between valence and conduction bands, new energy levels are formed. This is due to newly formed charge carriers. Upon further oxidation, two charge carriers are formed (radical dication or bipolaron) and energy levels come more closer to the mid energy gap. However, on a cyclic voltammogram, two separate peak resulting from formation of polaron and bipolarons can be rarely seen. Peaks are usually broad with high scan rates. To obtain more discernible voltammograms, voltammetry studies should be conducted with low scan rates [4].

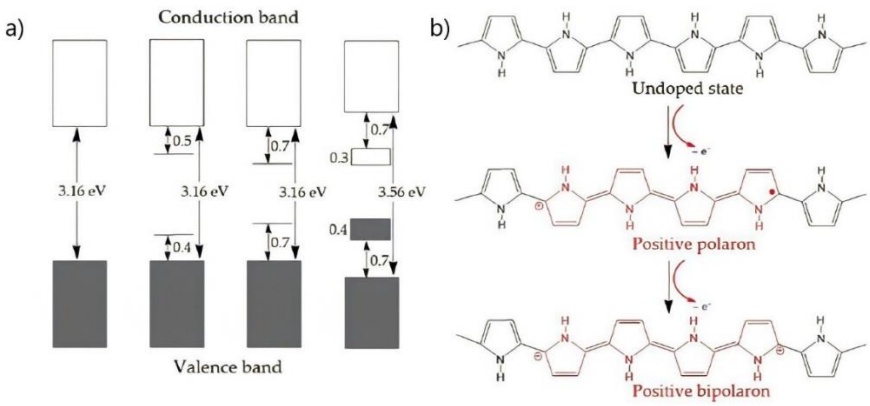

Figure 1.5. a) Valence and conduction band representation b) Illustration of doping process of PPy [3]

Since the band gap is a major factor in determining both the electrical conductivity and opto-electronic properties of a polymer, its control is crucial. For example, narrower bandgap results in a boosted thermal population of the conduction band; thus, both the number of charge carriers and electrical conductivity increases [16]. The band gap values of some common conjugated polymers are depicted in Figure 1.6.

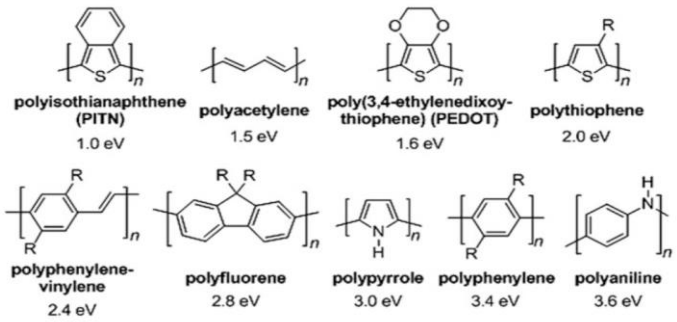

Figure 1.6. Bandgap values of some conjugated polymers [16]

The term “Band Gap Engineering” comes into play at this stage. In band gap engineering, understanding the factors that affect the band gap is very important. These factors are planarity, aromaticity energy, π-conjugation length, bond-length alteration and donor-acceptor (D-A) effect. Low bandgap polymers could be obtained by designing an aromatic backbone of the polymer planarly because π-electrons on the backbone delocalized to a higher degree when planarity is achieved [17]. Additionally, the alternation of single and double bonds in the polymer structure is usually one of the reasons for the low bandgap; thus, bond-length alternation which is the average lengths of single and double bonds, gains importance. Bandgap increases with increasing bond-length alternation. In order to reduce bandgap, using alternate donor and acceptor units is an effective way to reduce the difference in bond-length alternation. Two resonance forms [D-A and $D^{+}=A^{-}$] are acquired by applying the “Donor-Acceptor Approach” [18].

1.2.2 Donor-Acceptor Approach

Donor-Acceptor (D-A) alternating structure is one of the critical performance improvement method and most popular approach among others in the literature for tuning the bandgap (E_g) of the conducting polymer. The D-A approach was identified and explained firstly by Havinga and co-workers in 1992 [19]. They called the concept as "regular alternation of conjugated strong donor and acceptor-like moieties in a conjugated backbone". According to their approach, strong donor and acceptor moieties are needed, i.e., using weak donor and weak acceptor units in the alternate conjugated polymer backbone has not resulted in small band gap polymers [19]. [D-A and $D^+=A^-$] resonance form results in bond length alternation, and it leads to a decreased bandgap, i.e., this mesomerism and interaction between these two units increase the double bond character [16]. Frontier Orbital Theory has been used to explain HOMO-LUMO energy level separation in D-A systems. D-A dimer has a smaller bandgap than D-D or A-A dimers. Because of the difference between the characteristics of the donor and acceptor moieties electronically, "Intramolecular Charge Transfer" i.e. transition between donor unit and acceptor unit gains importance.

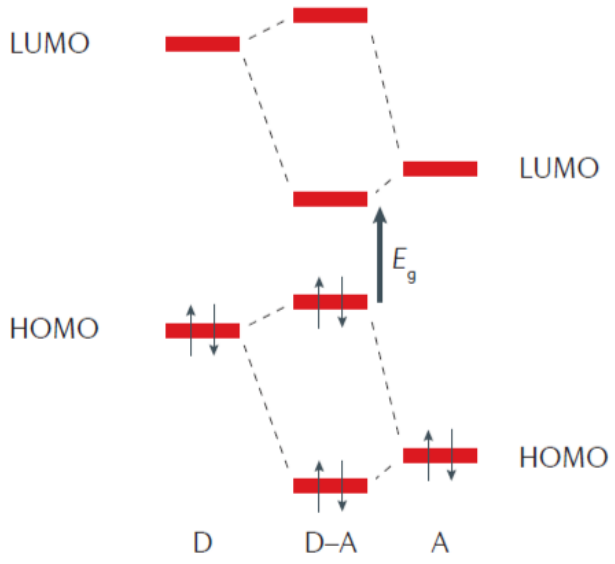

Figure 1.7. Molecular orbital representation of Donor-Acceptor approach

Hybridization of the energy levels of the donor and acceptor units yields new energy levels of D-A monomer with a small HOMO-LUMO energy separation. To enhance the electrochemical properties of the conjugated polymer, numerous combinations of donor and acceptor units have been used in the literature [20].

Lower energy absorption in donor-acceptor type materials is associated with the transition comes from the difference in electronic character between D-A units. Typically observed dual-band absorption of D-A type molecules has been explained by ICT phenomenon [16].

The D-A approach has been commonly used as a synthetic route to obtain low bandgap polymers. Donors are the electron-rich moieties with having high HOMO energy level and acceptors are the electron-deficient moieties with having low LUMO energy level. Electron donating or accepting–ability of these units can be monitored by introducing either electron-withdrawing or electron-donating groups to a molecule. Electron withdrawing unit can be an electronegative atom or an ion group having a formal positive charge like trifluoromethylsulfonyl, ammonium, nitro, sulfonyl, cyano, trihalomethyl, carboxyl, alkoxycarbonly, aminocarbonyl and halo groups. On the other hand, electron donating group can be identified by its lone electron pairs on the atom adjacent to the π-system like amino, hydroxy, alkoxy, acylamido and acyloxy groups [21]. Some common donor and acceptor groups are depicted in Figure 1.8.

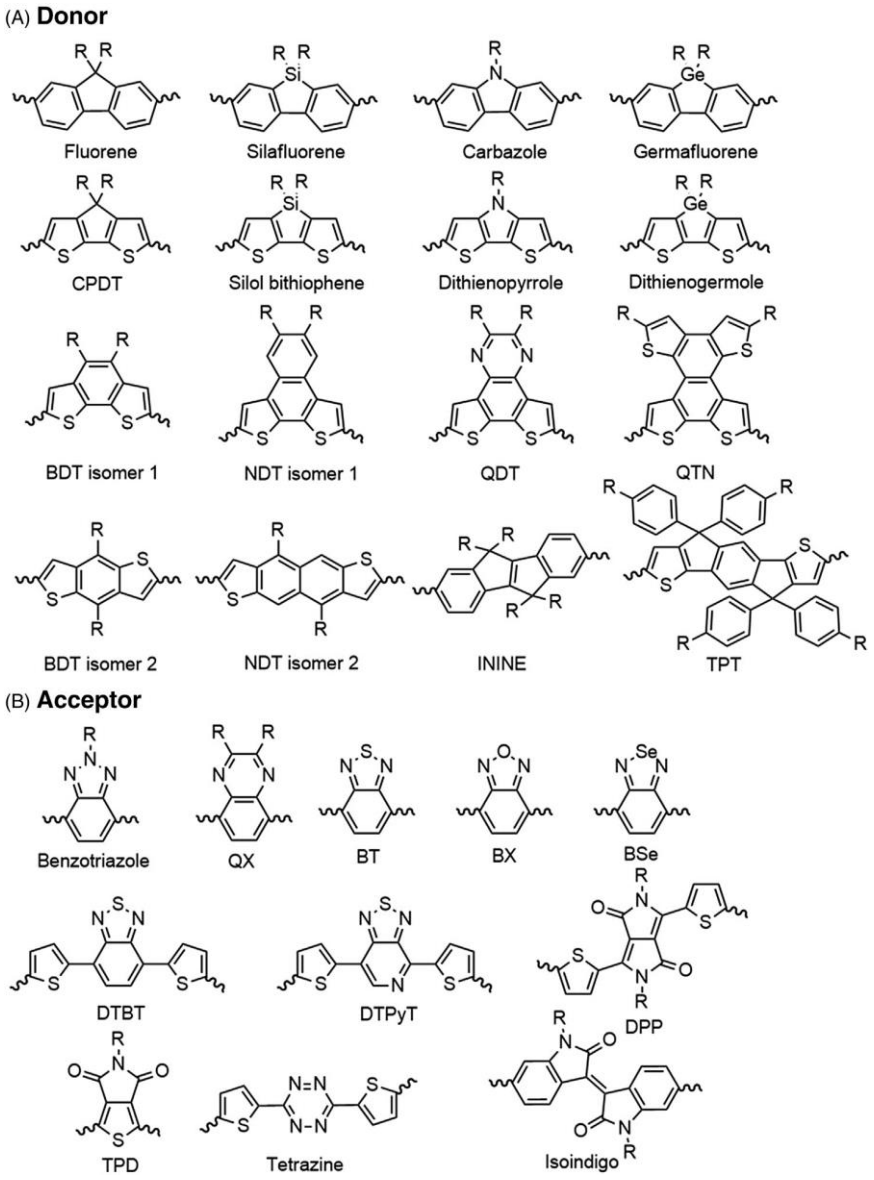

Figure 1.8. Typical a) donor and b) acceptor moieties [20].

1.3 Methods for Synthesizing Conjugated Polymers

In the field of conjugated polymers, there are several ways to achieve polymerization (Scheme 1.1). Each method of synthesis has several advantages or disadvantages. Scientists have to decide which method is the most appropriate way to obtain the desired polymer. For example, large scale production is possible during chemical polymerization. On the contrary, obtaining large amounts of polymer is not possible

when the electrochemical synthesizing method is chosen. However, thin-film preparation (up to 20 nm) is easier by electrosynthesis, and depositing the polymer as a film on the electrode substrate can be achieved during the polymerization [12].

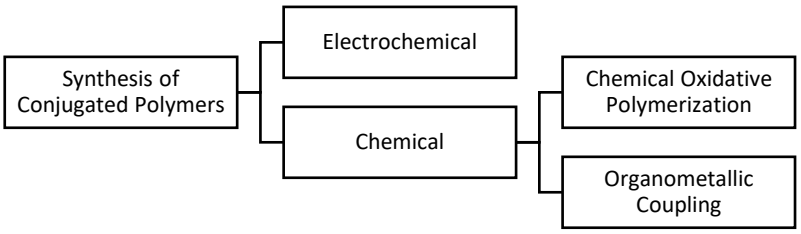

Scheme 1.1. Synthesis of conjugated polymers

Chemical polymerization can be divided into two as organometallic coupling and chemical oxidative polymerization. The organometallic coupling includes several methods such as McCullough, Rieke, GRIM, Suzuki Coupling, Stille Coupling, Cassar-Heck-Sonogashira Coupling, and Yamamato Coupling. Among those, Suzuki and Stille Coupling reactions are commonly used for the synthesis of D-A type monomers [20]. Catalytic cycle of transition metal catalysed coupling reactions and disproportionation reaction in the cycle is shown in Scheme 1.2.

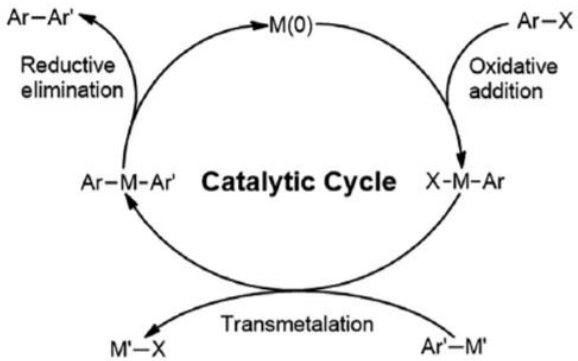

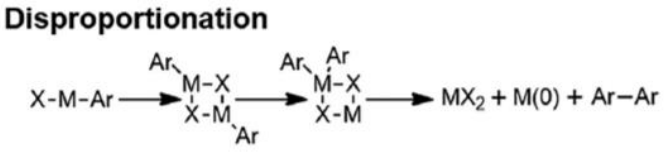

Scheme 1.2. General mechanism of catalytic cycle and disproportionation reaction in the catalytic cycle of the transition metal-catalysed synthesizing methods [20].

Suzuki and Stille couplings are the most preferred organometallic coupling reaction routes among others due to their superior advantages. Importantly, in these methods, experimental conditions are mild. Compared to Grignard reagents, Palladium catalysts are more stable to oxygen and water. Moreover, these methods have a higher tolerance for a great variety of functional groups [12].

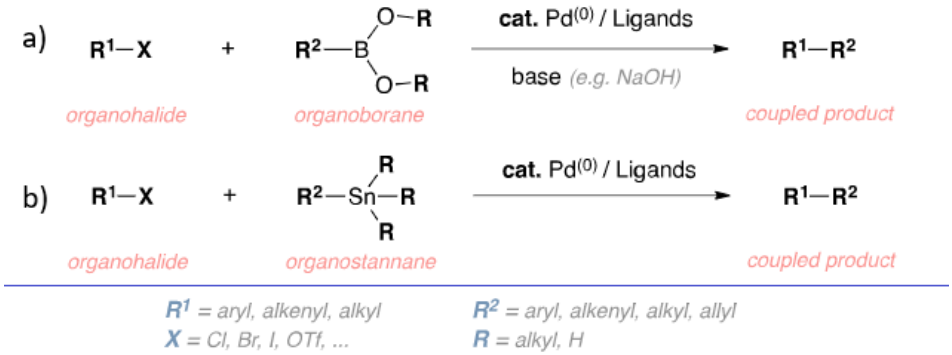

Scheme 1.3. Routes of a) Suzuki and b) Stille Cross-Coupling reactions

Chemical oxidative polymerization is based on the oxidation of a proper monomeric unit by the treatment with an oxidant such as $FeCl_3$ or $(NH_4)S_2O_8$.

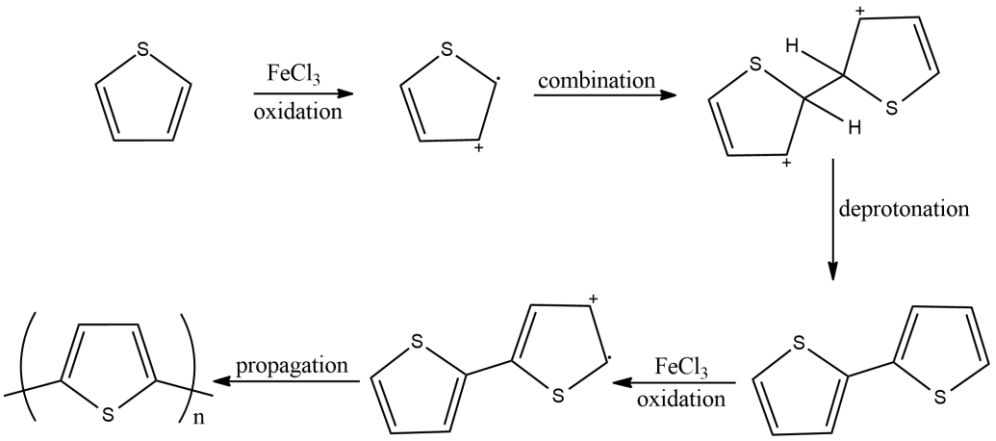

Scheme 1.4. Chemical oxidative polymerization with Ferric Chloride as an oxidant

Ferric chloride is the most commonly used oxidizing agent in the chemical oxidative polymerization and the generation of radical cation pairs takes place by oxidation of the monomer as shown in Scheme 1.4. After the radical cation formation, the polymerization reaction occurs by the following steps: the combination of the radical cations, deprotonation of the resulted dimer and so on, then finally propagation. Reaction conditions such as temperature, time, solvent, and amount of oxidizing agent should be carefully adjusted because these are the key factors that determine the final length and quality of the polymer [12].

1.3.1 Electrochemical Synthesis of Conjugated Polymers

In the electrochemical synthesis of conjugated polymers, a potential is applied to the solution containing the monomer and a suitable electrolyte. Three-electrode system consisting of working (WE), reference (RE) and counter (CE) electrode, is commonly used in the electropolymerization. Two types of three-electrode systems and representative voltammogram are shown in Figure 1.9. The electrodeposition of the polymer film takes place on the working electrode; in other words, the working electrode is the substrate during the electrosynthesis of the polymer. The working electrode itself should be inert and resistant to both oxidation and reduction.

Platinum, gold, tin(IV) oxide, indium tin oxide and stainless steel are the commonly used working electrode materials. Platinum or gold or, in some cases, glassy carbon or a metal foil can be selected as a counter electrode. Saturated calomel electrode and Ag/AgCl reference electrode systems are commonly used reference electrodes, latter is much more advantageous for aqueous or nonaqueous electrolytic systems [22].

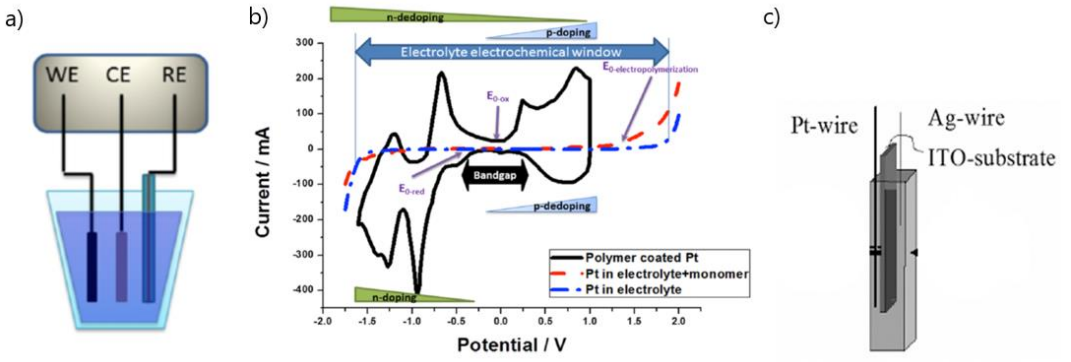

Figure 1.9. a)Electrochemical cell illustration of the three-electrode system b)Potential window of the electrolyte (blue line), oxidation of the monomer during polymerization (red line), and the voltammetric response of the doped conducting polymer (black line) [22]

Electrochemical cells are usually made up of glass, but for spectroelectrochemical studies, quartz cells should be preferred. Electrolyte solution, contains a dissociated salt, an acid or a base in a suitable solvent that is used for electrosynthesis of the polymers.

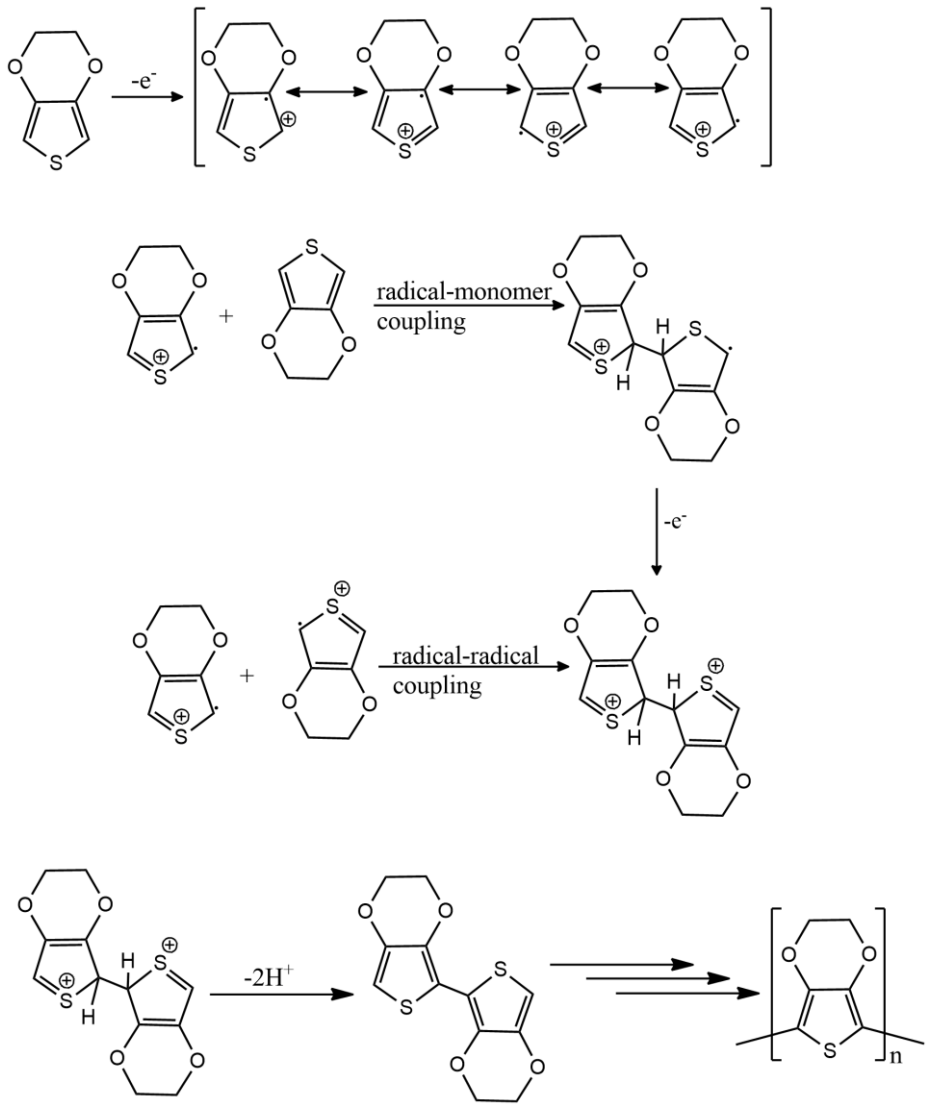

Scheme 1.5. Electrosynthesis mechanism of PEDOT [23]

During the electrosynthesis of a conjugated polymer, a coupling reaction takes place between previously initiated radical cations. Besides the radical-radical coupling, the radical-monomer coupling is also possible. By the loss of two protons, the reaction has resulted in the formation of a dimer. Another radical cation attacks to the dimer oxidized, then the polymerization proceeds via chemical and electrochemical ways and usually an insoluble oligomer deposition takes place on the working electrode

surface [23]. As a representative example, the electropolymerization mechanism of EDOT is given in Scheme 1.5.

During the electrosynthesis of the polymer film, specific parameters must be taken into account. Polymerization time, temperature, type and purity of the electrolyte (dopant), and the solvent choice of electrodes and the deposition load are the most critical factors that play a significant role in changing the morphology of the obtained film [22].

1.4 Determination of Bandgap (E_g) of Conjugated Polymers

Absorption measurements could be conducted for determining the bandgap of the polymer film. For this purpose, polymer is coated on transparent conducting substrates like indium tin oxide (ITO) coated glass electrode by physically or electrochemically, and then spectroelectrochemical studies are performed to monitor the changes in the electronic absorption spectra as shown in Figure 1.10. The bandgap, E_g, value obtained from the onset of lower energy absorption band (due to π-π^*) utilizing the following equation.

$$E_{g,optical}=\frac{1240}{\lambda_{onset}}$$

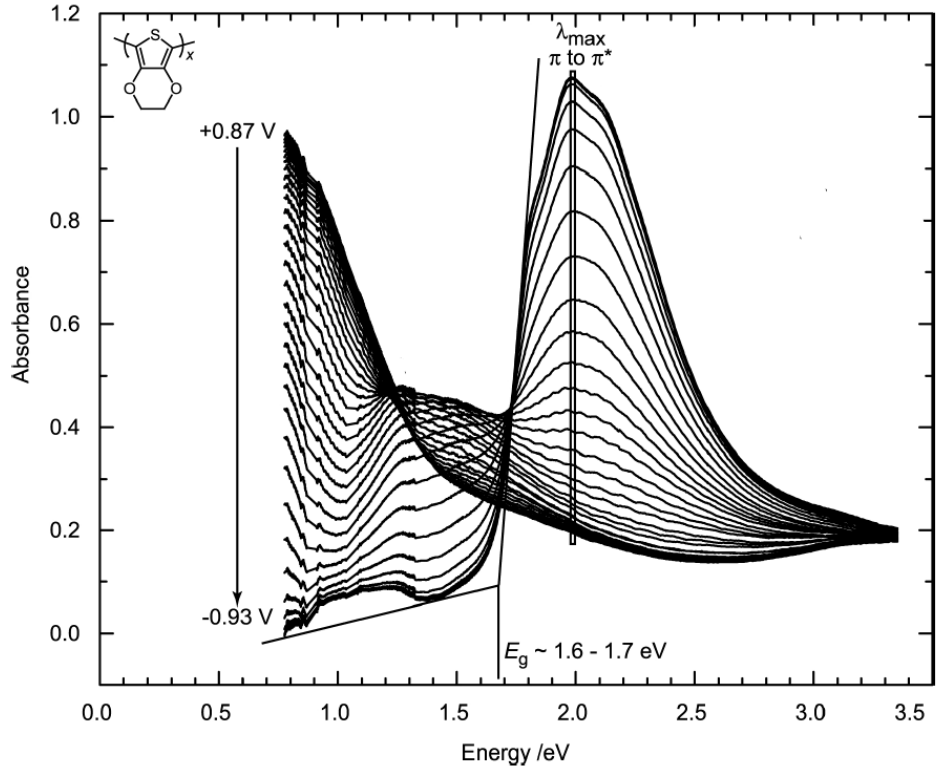

Figure 1.10. Absorption spectra of PEDOT film. [24]

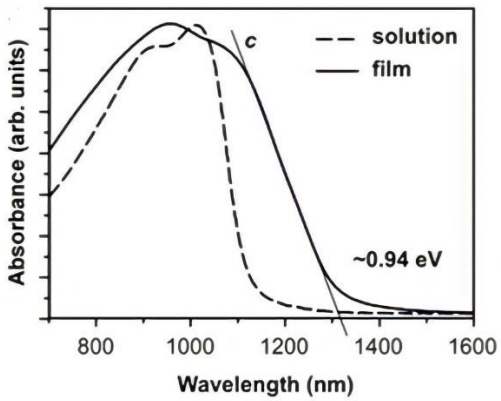

Figure 1.11. Determination of λ_{onset} by extrapolation of transition angle to the baseline [16]

Besides absorption measurements, electrochemical techniques such as Cyclic Voltammetry (CV) and Differential Pulse Voltammetry (DPV) techniques can also be preferred for the E_g determination [25]. By analyzing the voltammogram of the polymer film, the first reduction onset value (E^{red}_{onset}) and the first oxidation onset value (E^{ox}_{onset}) of the polymer are attained.

$$E_{g,electronic}=E^{ox}_{onset}-E^{red}_{onset}$$

The formula above shows how to calculate electronic bandgap value from these onset values. CV and DPV techniques provide more accurate and sensitive results because these methods minimize the capacitive current [25].

1.5 Electrochromism and Conjugated Polymers

Electrochromism is a redox driven reversible process that can be explained as colour and opacity change with respect to the applied electrochemical potential [26]. Viologens, metal oxides, coordination metal complexes, conjugated polymers are some examples of electrochromic materials studied in the literature [27].

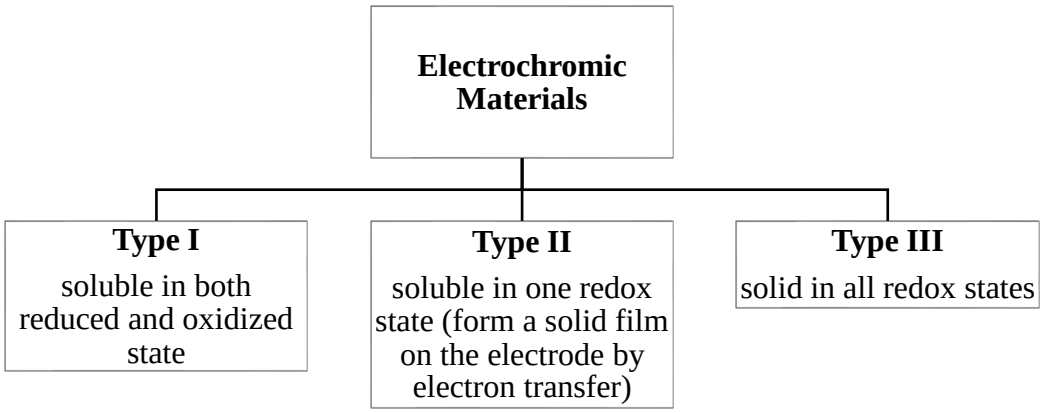

Scheme 1.6. Classification of electrochromic materials according to the solubility of redox state

According to solubility of each redox state, electrochromic material can be divided into three groups (See Scheme 1.6.). Conducting polymers are classified under Type III. Polyelectrochromism is observed when more than two oxidation-reduction states are electrochemically available with distinct electronic spectra. Many of the conjugated conducting polymers have this feature and bandgap (E_g) value of the polymer determines its electrochromic properties. For example, undoped thin films with E_g>3.0 eV absorbs at about 400 nm, on the other hand, thin films with 1.7 eV > E_g > 1.9 eV absorbs in the visible region at around 650-730 nm [27].

However, it is not enough to have electrochromic properties to be a good candidate for commercial electrochromic device applications. Several performance parameters have been defined: coloration efficiency, contrast ratio, switching speed, optical memory and electrochemical stability parameters indicate whether the resulting conducting polymer is suitable for an optoelectronic application or not [26,27].

1.6 Donor and Acceptor Units Used in This Study

1.6.1 Carbazole

Carbazole is a molecule that has attracted the attention of researchers for many years. Scientists frequently prefer this moiety because of its characteristic and advantageous features. Firstly, 9H-Carbazole is a very cheap and readily available starting material on the market. Remarkable environmental stability and good hole transporting ability of this moiety are associated with its fully aromatic backbone. Carbazole groups on the skeleton can easily form stable radical cations. Additionally, carbazole can be functionalized with a variety of groups that can be added onto the nitrogen atom. Structural modifications help researchers to modify the physical, electrical and optical properties of the moiety [28].

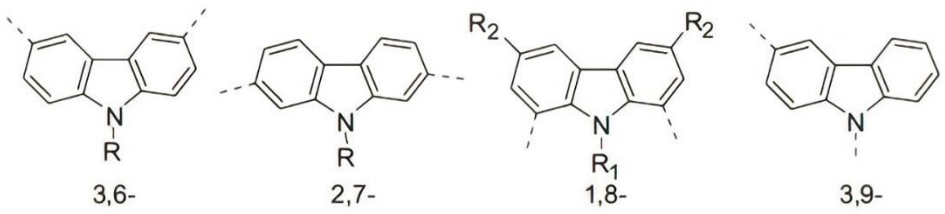

Figure 1.12. Carbazole derivatives

Carbazole derivatives used in conjugated conducting polymers are shown in Figure 1.12. Carbazole is a very advantageous moiety for scientists in the field of CPs. It can be used as both donor and acceptor and this affects the electrochromic properties of the monomer and its polymer. For example, when the carbazole unit is coupled with a strong donor such as 3,4-Ethylenedioxythiophene (EDOT) or 3,4-propylenedioxythiophene (ProDOT), the electrochromic properties of the resulting monomers and polymers draw attention. Obtained polymers have good stability (both optical and electrochemical), fast switching times and high coloration efficiencies [28]. Carbazole unit can also be coupled with strong acceptor groups such as benzothiadiazole as it is presented in this study. In this case, it acts as a donor. When 9H-Carbazole is coupled with 4,7-dibromo-2,1,3- benzothiadiazole, it results in a low-intensity absorption band [29] in the visible region due to ICT between carbazole and benzothiadiazole units. The effect of the connection site of the carbazole unit (2,7 or 3,6) has also been investigated. As an example, DPP(2,5-dihydro-3,6-di-2-thienyl-pyrrolo[3,4-c]pyrrole-1,4-dione) was coupled with both 2,7 and 3,6 carbazole and it is shown that 3,6-linked carbazole derivative has slightly lower E_g values and stronger ICT compared to 2,7-linked derivative [30].

1.6.2 2,1,3-Benzothiadiazole (B)

2,1,3-Benzothiadiazole (B) is one of the most frequently used molecules in the light technology of conjugated polymers. Due to its strong electron-withdrawing capacity,

compounds bearing this heterocyclic system are good candidates as electron carriers. Hence, B can be used as an electron acceptor unit for π-extended photoluminescent compounds. Conjugated materials such as small molecules, oligomers, or polymers containing B unit have high electron affinity and reduction potential usually. Moreover, B can be produced in large amounts with an easy procedure since it is a cheap material. Derivatization of B molecule is quite simple and its derivatives (See Figure 1.13.) such as quinoxalines and benzimidazoles are also good candidates for acceptor units in conducting materials [31].

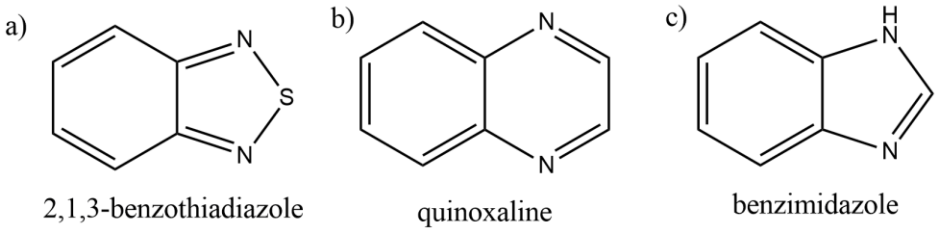

Figure 1.13. Chemical structures of a) 2,1,3-Benzothiadiazole, b)Quinoxaline, c)Benzimidazole

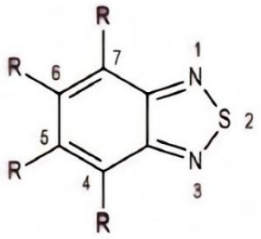

Figure 1.14. 2,1,3-Benzothiadiazole (B)

B can be functionalized from its sites shown in Figure 1.13-a. and heteroatom substituted derivatives, triple fused ring structures, tetracyclic structures and large π-extended B derivatives can be obtained (See Figure 1.15). Each benzothiadiazole derivative has its own advantage among other units. These acceptor building blocks are good candidates for optoelectronic applications. Because their effect on the

electrochemical behavior of the monomer and polymer is different, the B derivative to be used should be selected according to the application area [31]. Heteroatom substitution can be the most obvious example to show the importance of the choice of the derivative. As an example from the literature, EDOT monomer was coupled with 5-fluorobenzo[c][1,2,5]thiadiazole, 5,6-difluorobenzo[c][1,2,5] thiadiazole and 2,1,3-Benzothiadiazole. Fluorinated derivatives result in a blue shift in the electronic absorption spectra. Moreover, the fluorine atom lowers the HOMO level and thus increases the oxidation potential of the corresponding monomer [32].

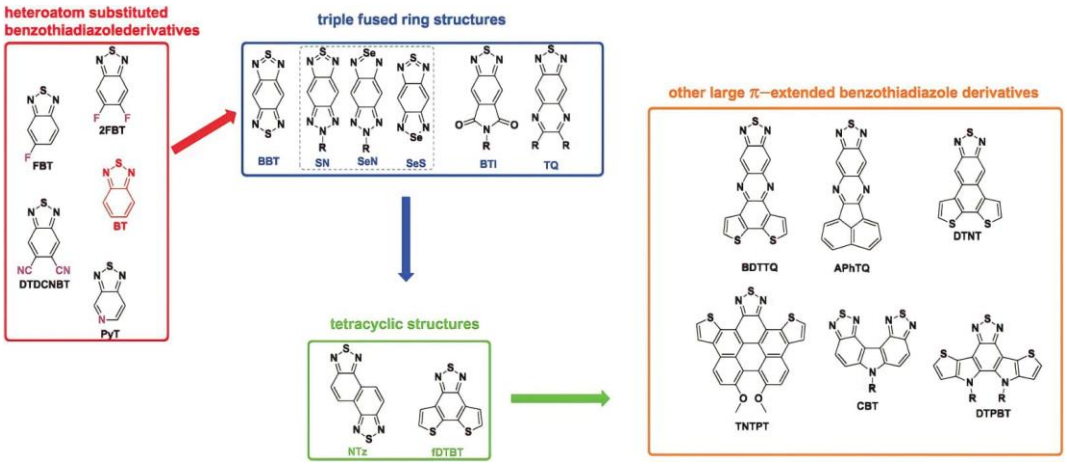

Figure 1.15. Common Benzothiadiazole derivatives in the literature [31]

1.7 Aim of the Study

More recently, D-A-D' type monomers has become more preferred than D-A-D type monomers due to having more redox sites as compared to D-A-D type monomers. As a result, number of metastable states increases which improves the electrochromic properties of their corresponding polymers. Usually, polymers obtained from monomers with asymmetric D-A-D' type structure have more visible color change [33]. The goal of this work is to investigate the effect of changing or combining the donor units symmetrically and unsymmetrically on the optical and electrochemical properties of the monomers and their polymers. For this reason, a new series of D-

A-D and D-A-D' type monomers were synthesized with different combinations of monomers. Thiophene (**T**) and 9-Benzyl-9*H*-carbazole (**C**) were used as donor units and 2,1,3-Benzothiadiazole (**B**) was used as an acceptor unit. To get information on the structure property relations, we have synthesized 4,7-bis(9-benzyl-9H-carbazol-3-yl)benzo[c][1,2,5]thiadiazole (**CBC**) and 4,7-bis(5-(9-benzyl-9H-carbazol-3-yl)thiophen-2-yl)benzo[c][1,2,5] thiadiazole (**CTBTC**) monomers. Moreover, to compare the effect of different units on the electrochemical and optical properties of the monomers we have also synthesized a D-A-D' monomer, namely 4-(9-benzyl-9H-carbazol-3-yl)-7-(thiophen-2-yl)benzo[c][1,2,5]thiadiazole (**CBT**). To complete the comparative investigation, we have also re-synthesized commercially available **TBT**. The monomers synthesized in this work (See Figure 1.16) were characterized utilizing Nuclear Magnetic Resonance (NMR) and High-Resolution Mass Spectroscopic techniques (HRMS). The electrochemical and optical properties of monomers were investigated in terms of different donor units combined to benzothiazole unit both symmetricaly and unsymmetricaly.

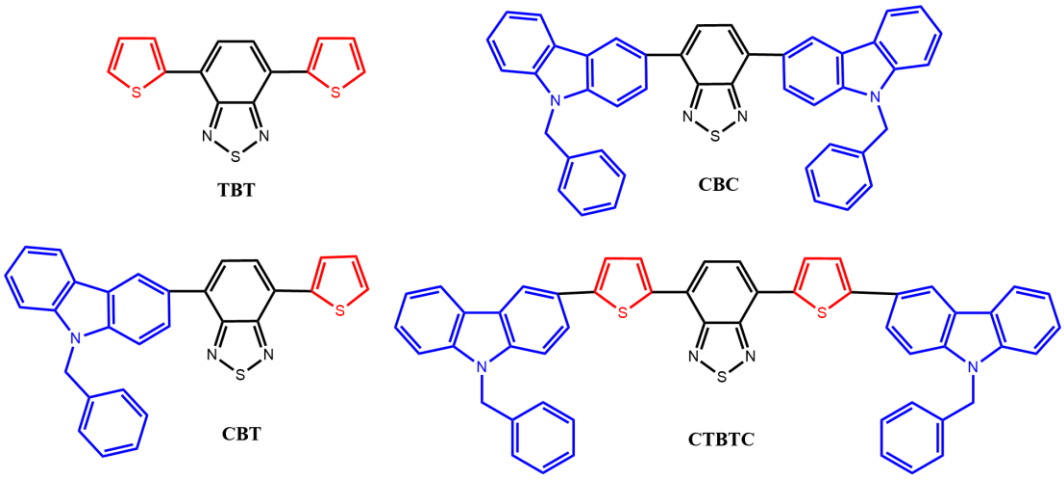

Figure 1.16. Structures of the monomers synthesized in this study

Furthermore, the monomers, **TBT**, **CBT**, **CBC**, and **CTBTC** were also were also polymerized potentiodynamically and opto-electronic properties of their polymers, namely P**TBT**, P**CBT**, P**CBC**, and P**CTBTC** were also investigated to further elucidate the effect of different donor units both in symmetrical and unsymmetrical sequence.

CHAPTER 2

EXPERIMENTAL

2.1 General

Chemicals used in synthesis are obtained from Sigma Aldrich except 4,7-di(thiophen-2-yl)benzo[c][1,2,5]thiadiazole, which was purchased from Derthon Optoelectronic Materials Science Technology Co LTD. Structures of the monomers were investigated via NMR spectroscopy with Bruker Spectrospin Avance DPX-400 Spectrometer. Tetramethylsilane (TMS) was used as an internal standard, and NMR spectra were recorded in $CDCl_3$ or DMSO-d_6. For the molecular weight determination of the synthesized monomers, Agilent 6224 Accurate-Mass TOF LC/MS instrument was used. All electrochemical studies were conducted with Gamry PCI4/300 Potentiostat/Galvanostat/ZRA combined with a suitable three-electrode system. As the WE/RE pairs, ITO (Delta Tech. 8–12, 0.7 cm×5 cm) coated quartz vs. Ag wire and Platinum disc vs. Ag/AgCl were used in the optical and electrochemical studies, respectively. The platinum wire was chosen as a counter electrode for both systems. Varian Cary Eclipse Fluorescence Spectrophotometer was used for recording the fluorescence spectra of the monomers. Agilent Cary 60 UV-Vis Spectrometer was used for conducting the optical measurements. Fluorescence quantum yields (QY) were calculated according to the data obtained by using Cary Eclipse Fluorescence Spectrophotometer. Perylene (QY=0.94; λ_{exc}=420 nm) and Rhodamine B (QY=0.65; λ_{exc}=520 nm) were utilized as the photoluminescence standards [34]. Solvents used in the synthesis, purification and characterization steps were freshly distilled before use.

2.2 Synthesis of Monomers

2.2.1 Synthesis of 4,7-bis(9-benzyl-9H-carbazol-3-yl)benzo[c][1,2,5]thiadiazole (CBC)

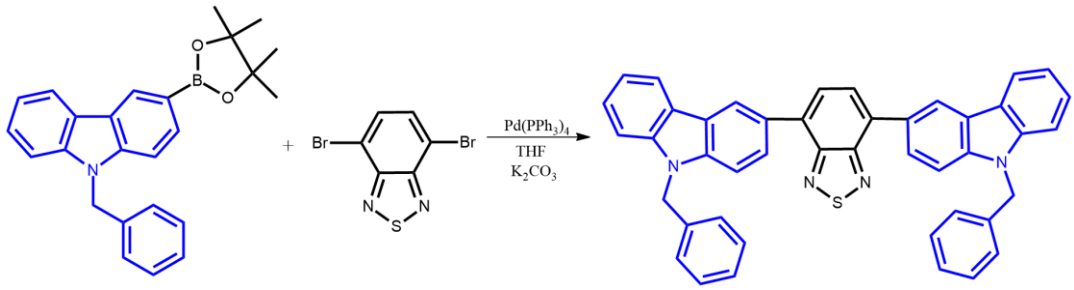

Scheme 2. 1. Chemical reaction route for synthesis of **CBC** monomer

Suzuki-Miyaura Cross-coupling reaction was achieved to synthesize the CBC monomer. Under an inert atmosphere, 4,7-dibromobenzo[c][1,2,5]thiadiazole (55.0 mg, 0.187 mmol) and 9-benzyl-3-(4,4,5,5-tetramethyl-1,3,2-dioxaborolan-2-yl)-9H-carbazole (150.0 mg, 0.391 mmol) were dissolved in 20 mL dry tetrahydrofuran in a two necked round bottom flask. Approximately 0.2 mL of aliquat 336 as a phase transfer catalyst and 1.0 mL of 2.0 M potassium carbonate in aqueous medium were added to the reaction mixture when the reaction temperature reached to 60 ^{o}C. After the reflux condition was obtained at 66 ^{o}C, tetrakis(triphenylphosphine)palladium(0) (30.0 mg, 0.026 mmol) was added then the reaction mixture was stirred for 36 hours at this temperature. The reaction process was controlled by thin-layer chromatography, and after the reaction was completed, tetrahydrofuran was evaporated under reduced pressure. Extraction of the crude product achieved with dichloromethane-water solvent system. The organic layer was dried over magnesium sulfate. The product was further purified by recrystallization over the chloroform-hexane solvent mixture. Then the solid orange product was filtered, and the residual solvent was removed. (Yield: 36%)

^{1}H NMR: ($CDCl_3$): 8.87 ppm (bs, 2H); 8.30 ppm (d, J = 7.6 Hz, 2H); 8.10 ppm (s, 2H); 8.18-8.15 ppm (dd, J = 8.4 Hz, 2H); 7.83 ppm (d, J = 8.6 Hz, 2H); 7.70 ppm (d, J = 8.2 Hz, 2H); 7.49 ppm (t, J = 7.4 Hz, 2H); 7.26 ppm (m, 12H); 5.77 ppm (s, 4H). ^{13}C NMR: 153.9; 140.6; 140.1; 137.7; 132.3; 128.6; 128.2; 128.1; 127.3; 126.8; 126.1; 122.5; 122.4; 121.1; 120.6; 119.3; 109. HRMS: (*m/z*) calculated for $C_{44}H_{30}N_4S$, $[M]^+$: 646.2191; found $[M]^+$: 646.2198.

2.2.2 Synthesis of 4-(9-benzyl-9H-carbazol-3-yl)-7-(thiophen-2-yl)benzo[c][1,2,5]thiadiazole (CBT)

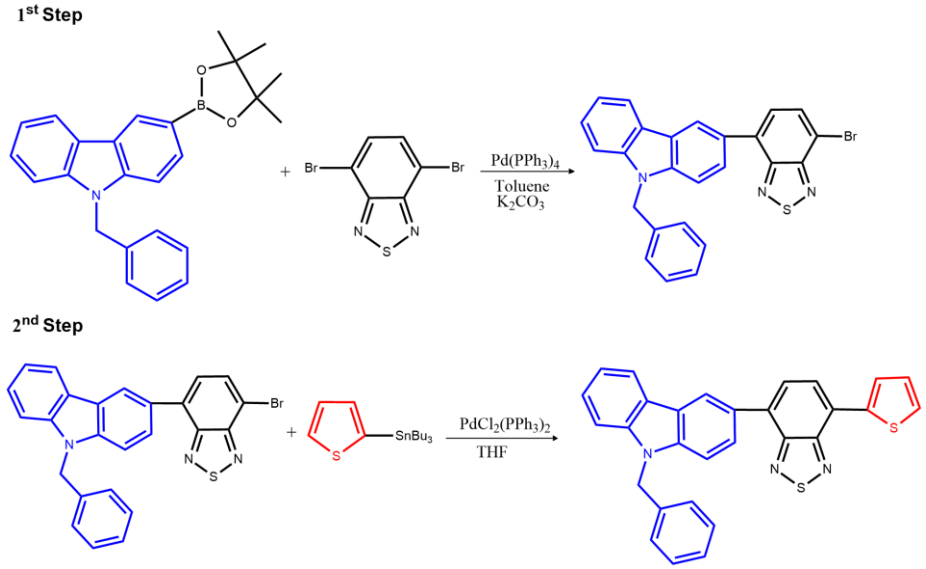

Scheme 2. 2. Chemical reaction route for synthesis of **CBT** monomer

For the synthesis of the CBT monomer, two-step reaction routes were followed. First, 1:1 ratio of 9-benzyl-3-(4,4,5,5-tetramethyl-1,3,2-dioxaborolan-2-yl)-9H-carbazole and 4,7-dibromobenzo[c][1,2,5]thiadiazole were reacted by Suzuki-Miyaura Cross-coupling then, this one side linked product was reacted with 2-(Tributylstannyl)thiophene via Stille cross-coupling reaction. Under an inert atmosphere, 4,7-dibromobenzo[c][1,2,5]thiadiazole (84.6 mg, 0.288 mmol) and 9-benzyl-3-(4,4,5,5-tetramethyl-1,3,2-dioxaborolan-2-yl)-9H-carbazole (100.0 mg,

0.262 mmol) were dissolved in 25 mL of dry toluene. After the reflux condition was obtained, approximately 0.2 mL of aliquat 336 as a phase transfer catalyst and 2.0 mL 2.0 M potassium carbonate in aqueous medium were added. Then, tetrakis(triphenylphosphine)palladium(0) (30.0 mg, 0.026 mmol) was added to the reaction mixture. The course of the reaction was monitored by thin-layer chromatography. After refluxing overnight in an inert atmosphere, the reaction was finished. The solvent was evaporated under reduced pressure, and the product was extracted with dichloromethane/brine mixture. Under reduced pressure, organic layer was dried. In the following second step, obtained one side linked carbazole derivative was coupled with 2-(Tributylstannyl)thiophene (196 mg, 0.524 mmol). Reaction mixture was refluxed with bis(triphenylphosphine)palladium(II)dichloride(Pd(II)) (30 mg, 0.043 mmol for two days. Purification of the product was achieved by column chromatography with the solvent system of hexane/ethyl acetate (50:1) mixture as an eluent (Yield: 41%).

^{1}H-NMR: ($CDCl_3$): 8.65 ppm (d, J=1.6 Hz, 1H); 8.15 ppm (d, J=7.6 Hz, 1H); 8.07 ppm (dd, J=4.7 Hz, 1H); 7.99 ppm (d, J=1.7 Hz, 1H); 7.97 ppm (d, J=1.7 Hz, 1H); 7.91 ppm (d, J=7.5 Hz, 1H); 7.75 ppm (d, J=7.4 Hz, 2H); 7.46 ppm (s, 1H); 7.44 ppm (s, 1H); 7.40 ppm (m, 3H); 7.35 ppm (s, 1H); 7.23 ppm (s, 1H); 7.21 ppm (m, 2H); 5.51 ppm (s, 2H). ^{13}C-NMR: 154.4; 153.0; 141.2; 140.7; 139.7; 137.0; 133.9; 128.9; 128.6; 128.0; 127.7; 127.6; 127.3; 127.3; 126.5; 126.2; 125.6; 123.5; 123.3; 121.3; 120.7; 119.6; 109.2; 109.0; 46.8. HRMS: (*m/z*) calculated for $C_{29}H_{19}N_3S_2$, $[M]^+$: 473.1020; found $[M]^+$: 473.1030

2.2.3 Synthesis of 4,7-bis(5-(9-benzyl-9H-carbazol-3-yl)thiophen-2-yl)benzo[c][1,2,5] thiadiazole (CTBTC)

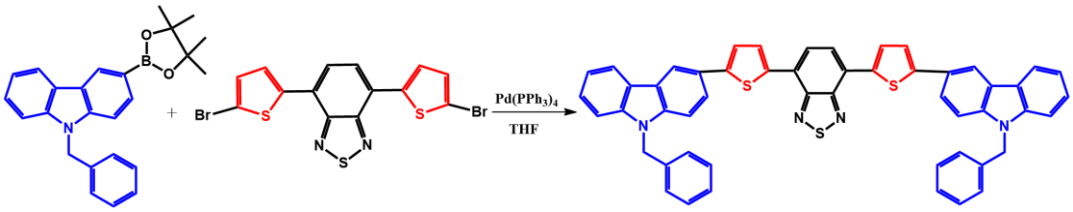

Scheme 2. 3. Chemical reaction route for synthesis of **CTBTC** monomer

CTBTC monomer synthesis was achieved by Suzuki-Miyaura Cross-coupling reaction in which 4,7-bis(5-bromothiophen-2yl)benzo[c][1,2,5]thiadiazole were coupled with 9-benzyl-3-(4,4,5,5-tetramethyl1,3,2-dioxaborolan-2-yl)-9H-carbazole. Under an inert atmosphere, 4,7-bis(5-bromothiophen-2-yl)benzo[c][1,2,5]thiadiazole (70.0 mg, 0.153 mmol) and 9-benzyl-3-(4,4,5,5-tetramethyl-1,3,2-dioxaborolan-2-yl)-9H-carbazole (100.0 mg, 0.261 mmol) were dissolved in 20 mL of dry tetrahydrofuran. When the reaction reached the reflux condition, 0.4 mL of Aliquat 336, 2.0 mL of potassium carbonate aqueous solution (2.0 M) and lastly Tetrakis(triphenylphosphine)palladium(0) (30.0 mg, 0.026 mmol) were added to the reaction mixture. After the synthesis was conducted in reflux condition for 24-hours, the reaction was ended up according to thin layer chromatography. Then, the solvent in the reaction medium was evaporated and product was extracted with Chloroform/Brine mixture. The organic phase was dried over magnesium sulfate. Column chromatography and recrystallization was preferred for further purification of the crude product with the solvent mixtures of chloroform/hexane (3:2) and dichloromethane/acetonitrile respectively. (Yield: 29%)

^{1}H-NMR: (DMSO-d_6): 8.65 ppm (d, J=1.3 Hz, 2H); 8.34 ppm (d, J=7.6 Hz, 2H); 8.26 ppm (d, J=3.9 Hz,2H); 8.20 ppm (s, 2H); 7.90 ppm (d, J=8.5 Hz, 2H); 7.74 ppm (m, 4H); 7.67 ppm (d, J=8.3 Hz, 2H); 7.48 ppm (t, 2H); 7.25 ppm (m, 12H); 5.66

ppm (s, 4H). 13C-NMR: 152.7; 147.0; 141.2; 140.5; 137.0; 129.0; 128.9; 128.7; 128.2; 127.6; 126.4; 126.3; 125.9; 125.7; 125.2; 124.3; 123.1; 120.7; 119.6; 117.9; 109.3; 109.2; 100.0; 96.8; 96.2; 46.7. HRMS: (*m/z*) calculated for $C_{52}H_{34}N_4S_3$, $[M]^+$: 810.1946; found $[M]^+$: 810.1944

CHAPTER 3

RESULTS AND DISCUSSION

In this study, a new series of D-A-D and D-A-D' type bearing 2,1,3-Benzothiadiazole (**B**) as the acceptor unit were synthesized. 9-benzyl-9H-carbazole (**C**) and 9H-carbazole-thiophene (CT) were used as the donor units. In order to further out our knowledge on the structure property relationship of monomers, **CBC** and **CTBTC** were synthesized via Suzuki cross-coupling reactions. To complete the comparative investigation, we have also re-synthesized commercially available **TBT**. Since asymmetric D-A-D' type monomers and their polymers reported to exhibit more redox sites and enriched electrochromism [33], we have also synthesized an asymmetric D-A-D' type monomer using **C** and **T** as donor units (**CBT**) to compare the effect of different units on the electrochemical and optical properties of the monomers.

3.1 Optical and Electrochemical Properties of the Monomers

In order to inspect the effect of different donor units on the optoelectronic properties of **TBT**, **CBT**, **CTBTC** and **CBT**, firstly their electronic absorption and fluorescence emission spectra were recorded in dichloromethane (DCM) and the results are given in Figure 3.1. As it is seen from the figure, all the monomers displayed characteristic dual absorption band due to the donor-acceptor pattern. The one that appear at higher energy (short wavelength) is due to $\pi \rightarrow \pi^*$ and the lower energy band can be attributed to itramolecular charge transfer (ICT). The $\pi \rightarrow \pi^*$ transition bands arise at 300 nm for **TBT**, **CBT** and **CBC**. On the other hand, this band appears at about 347 nm in the case of **CTBTC**. This red shift in the $\pi \rightarrow \pi^*$ band is most probably due to increased conjugation in the five membered **CTBTC** monomer. A close inspection of Figure 3.1 reveals that there is a slight blue shift upon changing the

donor unit of the D-A-D type monomers from thiophene (for **TBT** 446 nm) to carbazole (for **CBC** 436 nm). Electronic absorption spectra of the monomers were also recorded in solvents of different polarities (i.e. hexane; ε=1.9, DCM; ε=8.9 and DMSO; ε=46.7) to confirm if the lower energy absorption band is due to ICT or not. Although almost no change was observed in the position of higher energy absorption band, a slight red shift with increasing solvent polarity was noted for lower energy absorption bands of the monomers. In the case of **TBT**, for example, this band shifts from 446 nm to 583 nm upon changing the solvent from hexane to DMSO. Similar red shifts were also observed for the other three monomers (See Table 3.1), **CBC**, **CBT** and **CTBTC**, confirming that the low energy band is due to ICT. For **CTBTC**, on the other hand, ICT band undergoes a remarkable red shift (λ_{max}=522 nm in DCM and (λ_{max}=539 nmin DMSO) indicating strongest ICT among others. The reason for this greater red shift might be due to the presence of thiophene π-conjugated spacers between the **B** and **C** units [35].

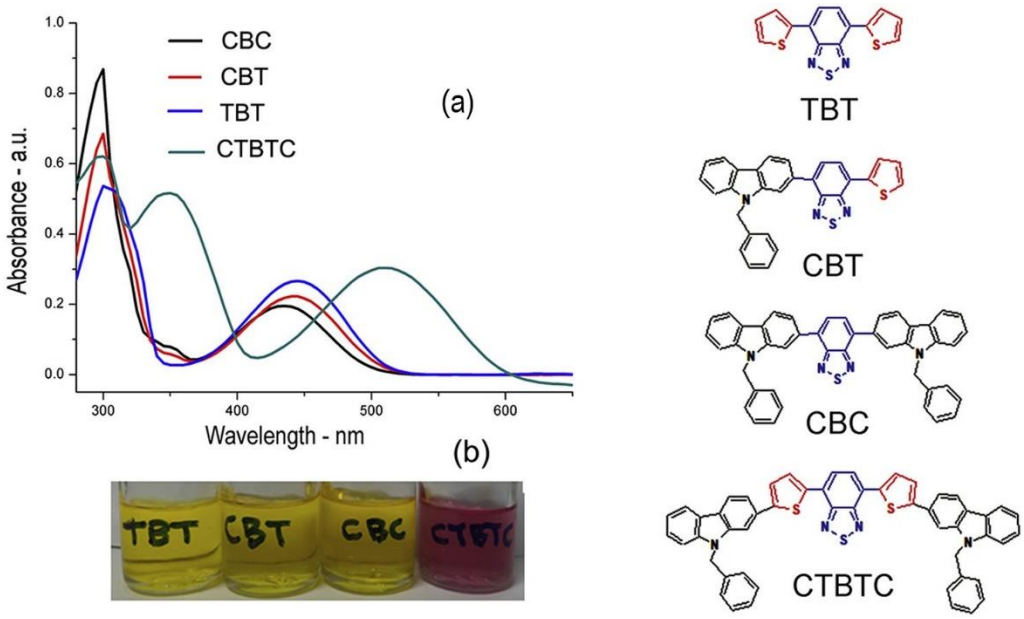

Figure 3.1. Structures of the monomers synthesized and a)UV-Vis spectra of the monomers in DCM solvent b) monomer solutions under daylight

The emission spectra of monomers were also recorded in solvents of different polarities to further confirm that the longer wavelength absorption band in the electronic absorption spectra of monomers are due to ICT and the emission spectra recorded in different solvent are depicted in Figure 3.2 a- d for **CBC**, **CBT**, **TBT** and **CTBTC**, respectively. The resulting emission maximum values are listed in Table 3.1 together with calculated Stoke's shift values.

A close inspection of Table 3.1 indicated that the emission spectra of monomers exhibit more pronounced bathochromic shift and increasing Stoke's shift with increasing solvent polarity. The larger red shift observed in the emission spectra of the monomers as compared to their absorption spectra indicates not only larger ICT and dipole moment of excited state as compared to the ground state [36] but also indicates the conformational changes of the molecules upon excitation (See Table 3.1.) [37]. This trend also can be seen in the photographs of the monomer solutions recorded under UV-light (Figure 3.1.). Moreover, fluorescence quantum yields of the monomers were also measured in DCM and found to be 0.48 for **CBC**, 0.46 for **CBT**, 0.55 for **TBT** and 0.55 for **CTBTC**.

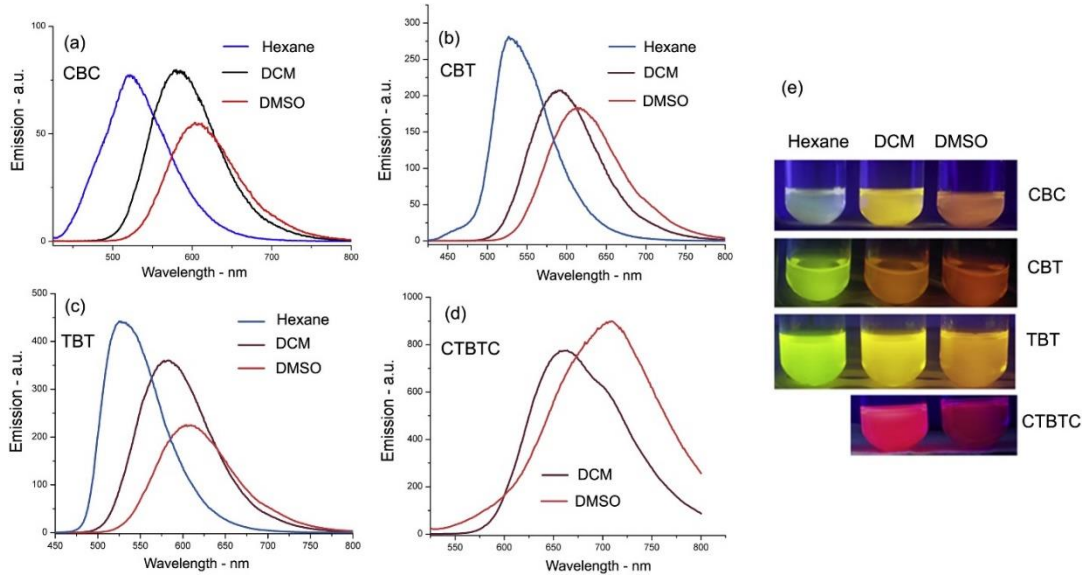

Figure 3.2. Fluorescence spectra of the monomers in Hexane, DCM and DMSO a)**CBC**, b) **CBT**, c) **TBT** , d) **CTBTC** e) monomer solutions in different solvents under UV light

Table 3.1. Optical properties of monomers in various solvents

Monomer	λ_{abs}[a]	λ_{emis}[a]	Stoke's Shift[a]	λ_{abs}[b]	λ_{emis}[b]	Stoke's Shift[b]	λ_{abs}[c]	λ_{emis}[c]	Stoke's Shift[c]	$E_{g\text{-}opt}$[b]	QY[e]
TBT	446	528	82	446	583	137	452	608	156	2.43	0.55
CBT	442	528	86	444	591	147	450	614	164	2.45	0.46
CBC	429	521	92	436	581	145	442	604	162	2.49	0.48
CTBTC	–[d]	–[d]	–[d]	522	661	135	539	709	170	2.06	0.55

a) in Hexane,
b) in DCM,
c) in DMSO,
d) insoluble,
e) in DCM with Rhodamine B as standard for **CTBTC** and with Pyrene as standard for **TBT**, **CBT**, and **CBC**

Prior to electrochemical polymerization of monomers, their electrochemical behaviors were investigated by using cyclic voltammetry (CV) technique in 0.1 M tetrabutylammonium tetrafluoroborate ($TBABF_4$) as the supporting electrolyte dissolved in DCM and the resulting voltammograms are given in Figure 3.3. The monomers synthesized in this work exhibit two quasi reversible oxidation peaks at 0.81 V and 1.24 V for **CTBTC**, 1.20 and 1.57 V for **CBT** and 1.19 V and 1.50 V for

CBC. The lower oxidation potential of **CTBTC** as compared to **CBC** and **CBT** might be due to increased π-conjugation in the five membered monomeric system.

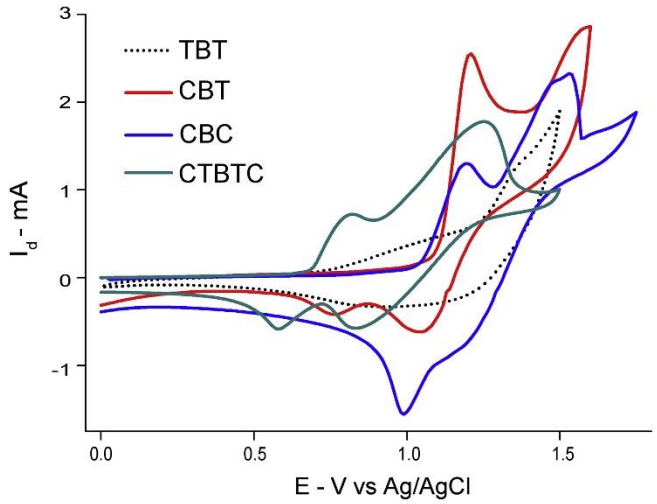

Figure 3.3. Cyclic voltammograms of **TBT**, **CBT**, **CBC** and **CTBTC** monomers (in 0.1 M $TBABF_4$-DCM)

To calculate the bandgap energy (E_g) of the monomers more precisely, differential pulse voltammetry (DPV) technique was used. The data were collected both in the cathodic and anodic regions in DCM containing 0.1 M $TBABF_4$ as supporting electrolyte. All DPVs which are shown in Figure 3.4 were recorded under inert atmosphere at room temperature. As depicted in Figure 3.4, the oxidation potentials are consistent with the results obtained from CV measurements (i.e. lowest oxidation potential for **CTBTC**). E_g values were evaluated from onset oxidation and reduction potentials as depicted in Figure 3.4 and the results are tabulated in Table 3.2 together with measured oxidation/reduction potentials. Among the monomers synthesized in this work **CTBTC** was found to exhibit lowest E_g value in accordance with the increased π-conjugation.

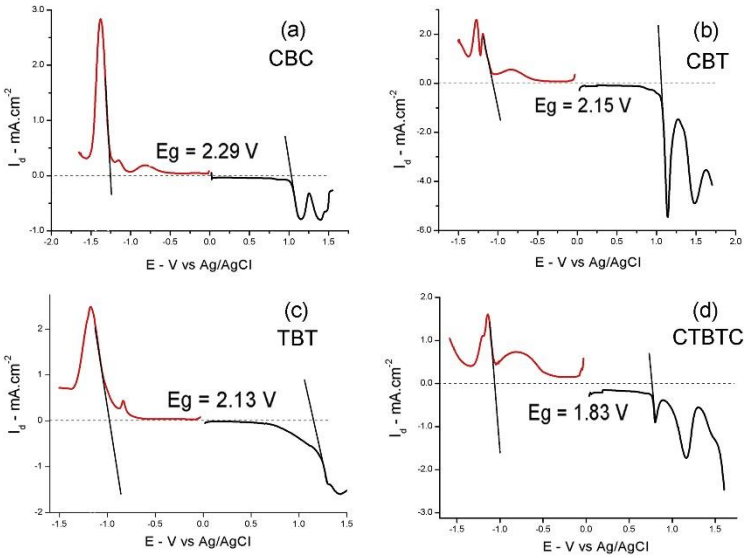

Figure 3.4. Differential pulse voltammograms of the monomers recorded in 0.1 M $TBABF_4$ electrolytic medium during n-doping and p-doping in the voltage range of a)-1.65 and 1.65V for **CBC** monomer b) -1.50 and 1.65 V for **CBT** monomer c) -1.50 and 1.50 V for **TBT** monomer d) -1.60 and 1.65 V for **CTBTC** monomer.

Table 3.2. Electrochemical properties of monomers

Monomers	E_{ox}[a] (V)	$E_{ox\text{-}onset}$[b] (V)	$E_{red\text{-}onset}$[b] (V)	$E_{g\text{-}elec}$[b] (V)
TBT	1.35	1.15	-0.98	2.13
CBT	1.20/1.57	1.06	-1.09	2.15
CBC	1.19/1.50	1.03	-1.26	2.29
CTBTC	0.81/1.24	0.77	-1.06	1.83

a) From CV
b) From DPV

3.2 Electrochemical Polymerization of CBT, CBC, and CTBTC

After electrochemical and optical characterization of the monomers, to investigate the effect of different donor units on the electrochemical and optical properties of

polymer films, we have tried to obtain their corresponding polymer films (i.e. P**CBT**, P**CBC**, and P**CTBTC**). For this purpose, monomers, except TBT, were dissolved in DCM containing 0.1 M $TBABF_4$ and this solution subjected to repetitive cycling within the predetermined potential range. Since the polymer film of **TBT** (P**TBT**) was already reported previously its polymer film was not prepared in this study and previously reported data was used for comparison purpose [38].

In the case of **CBC**, no sign of polymerization was observed during repetitive cycling between 0.0 V to 1.5 V vs Ag/AgCl in DCM -$TBABF_4$ electrolytic solution. Since changing the solvent-electrolyte couple, working electrode or potential range did not result any reasonable film formation we turned our attention to the electropolymerization of **CBT**, and **CTBTC**.

Contrary to **CBC**, **CBT** and **CTBTC** were successfully polymerized via repetitive cycling and the formation of the polymer films on the working electrode was observed. New redox couples frequently intensified during repetitive cycling, indicating polymer film formation on the working electrode surface. As depicted in Figure 3.5, electropolymerization of **CBT** was achieved during repetitive potential cycling in the potential range of 0.0 V and 1.5 V vs Ag/AgCl with a scan rate of 100 mV/s. In the case of **CTBTC** potential range was adjusted as 0.0 V to 1.65 V vs Ag/AgCl. After certain number of potential cyclings, the polymer film coated working electrode removed from the electrolysis cell and the surface of the polymer film was washed with DCM to remove any remaining electrolyte and unreacted monomers and oligomers. The electrochemical behavior of polymer films was investigated in monomer free electrolytic solution by recording their cyclic voltammograms in the potential range of 0.0 V and 1.5 V vs Ag/AgCl with the scan rate of 40 mV/s. Resulting voltammograms of P**CBT** and P**CTBTC** are demonstrated in Figure 3.5 c. As it is seen from the voltammograms both polymer films exhibited reversible oxidation peaks at about 1.09 and 1.34 V for P**CBT**, and at about 0.70 and 1.10 V for P**CTBTC**. On the other hand, P**TBT** exhibited one quasi-reversible oxidation peak at about 1.3 V vs Ag/AgCl [38]. Oxidation onset potentials of the polymer films followed the same trend (0.80 V for PCBT, 0.71 V

for P**TBT** and 0.65 V for P**CTBTC**) as in the case of their corresponding monomers reflecting the increasing effect of conjugation.

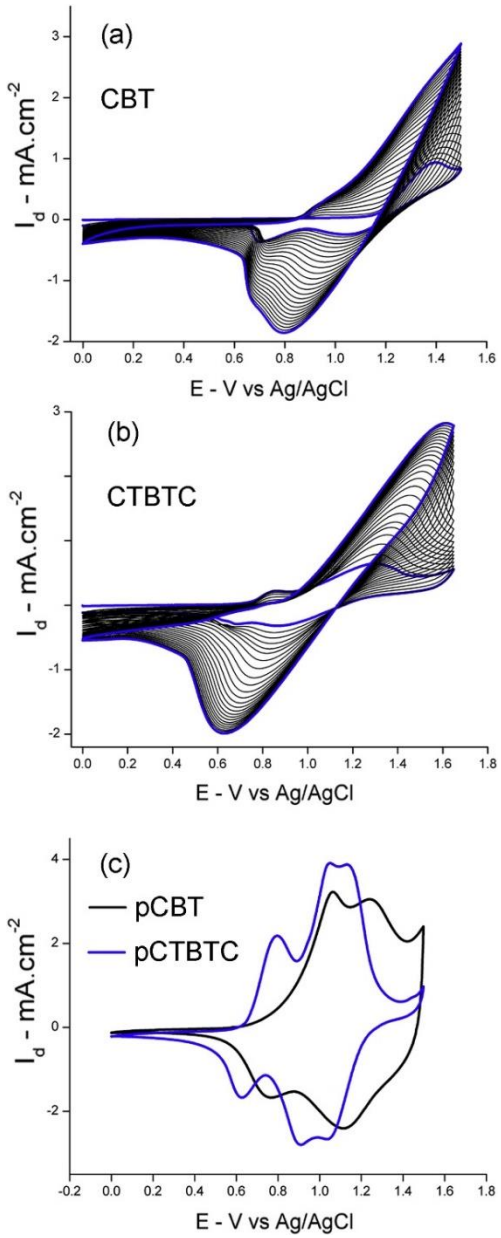

Figure 3.5. Cyclic voltammograms of the monomers during electropolymerizations of a) **CBT** (between 0.0 V and 1.5 V) b) **CTBTC** (between 0.0 and 1.65 V) in 0.1 M $TBABF_4$/DCM electrolytic medium studied with the scan rate of 100 mV/s. c) cyclic voltammogram of the resulting polymer films at a scan rate of 40 mV/s.

Scan rate dependence of oxidation and reduction current densities were also investigated by recording the cyclic voltammograms of polymer films at different scan rates between 20 mV/s and 140 mV/s with 20 mV increments (Figure 3.6). Both P**CBT** and P**CTBTC** films showed a linear relationship in its anodic/cathodic current densities as a function of scan rate, indicating a well adhered polymer film on the working electrode surface, as well as a non-diffusion controlled redox processes (Insets of Figure 3.6).

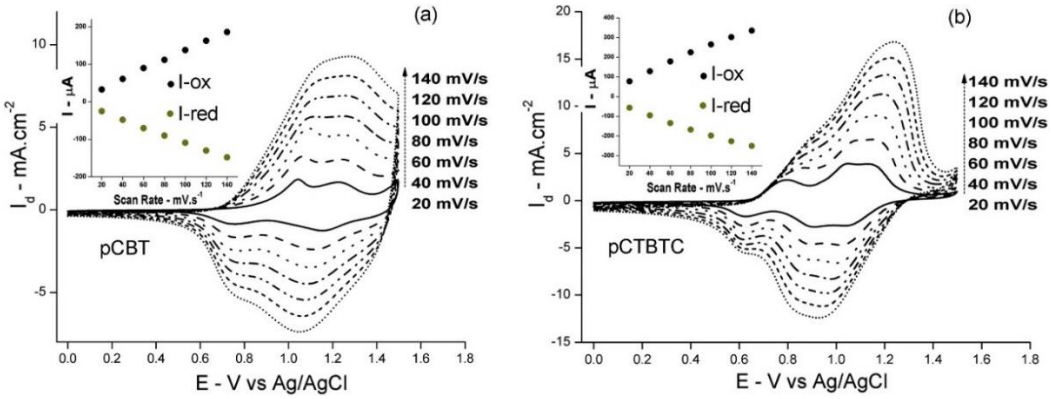

Figure 3.6. Scan rate dependence of a) PCBT and b) PCTBTC between 0.0 V and 1.50 V, at the scan rates from 20 mV/s to 140 mV/s with 20 mV increments. Insets: The anodic and the cathodic peak currents of polymer films vs. scan rate.

The electrochemical stability of the P**CBT** and P**CTBTC** polymer films were also tested. For this purpose, polymer films were cycled between neutral and oxidized states for 100 times. As shown in Figure 3.7, PCBT exhibited better electrochemical stability than P**CTBTC**. P**CBT** maintained about 85 % of its electroactivity after 100 cycling between 0.0 V and 1.5 V, on the other hand, P**CTBTC** lost 38 % of its electroactivity even after 10 cycles, indicating poor electrochemical stability which might be due to dissolution of the polymer film in the electrolytic medium.

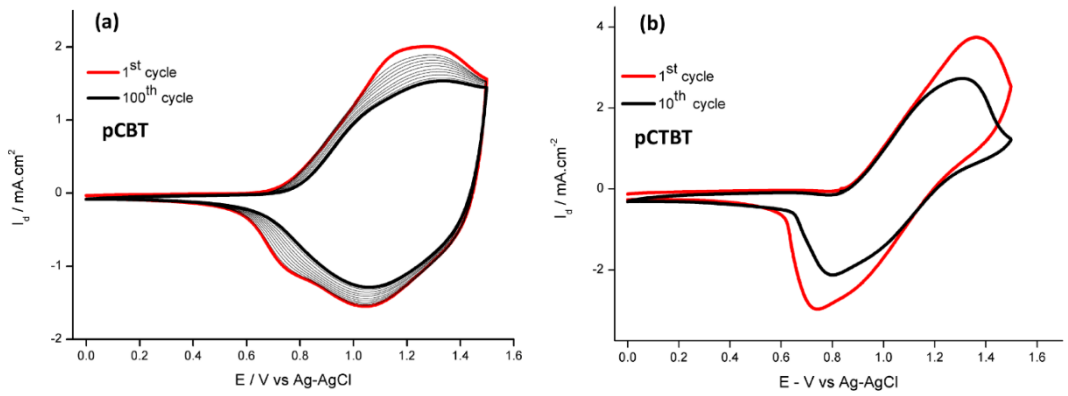

Figure 3.7. Cyclic voltammograms of polymer films upon many cycles a) P**CBT** upon 100 cycles, b) P**CTBTC** upon 10 cycles.

3.3 Optical Properties of the Polymer films PCBT and PCTBTC

Spectroelectrochemical studies were conducted after the deposition of P**CBT** and P**CTBTC** films on ITO transparent working electrode. Five repetitive cycles resulted in fine polymer films on the working electrode surface. The films were washed with ACN and then polymer film coated ITO working electrodes were placed in a monomer-free electrolytic solution of 0.1 M $TBABF_4$ in ACN. Change in the electronic absorption spectrum of each polymer films were monitored during a slow anodic scan (20 mV/s) and the resulting absorption spectra are shown in Figure 3.8.

In the neutral state maximum of the optical absorption band was measured at 530 nm for P**CBT** (Figure 3.8a). During oxidation from 0.0 V to 1.5 V, this band lost its intensity which is accompanied with the formation of a new band at about 730 nm, indicating the formation of charge carriers (or polarons). Appearance of a broad band beyond 800 nm, upon further oxidation, might be attributed to the formation of bipolarons. It is also worth to mention that P**CBT** film changed its neutral pale-pink colour to greenish-blue beyond 0.80 V.

As for P**CTBTC**, multichromic behaviour was observed during oxidation, which was clearly monitored by its UV-Vis spectra (Figure 3.8b). Neutral absorption band of P**CTBTC** gave its maximum at 576 nm and intensity of this band decreased with

the formation of a new band having maximum at 675 nm. During the formation of this new band, the neutral state pinky colour of the polymer film turned to green between 0.30 V and 1.2 V. Upon further oxidation (beyond 1.20 V), another band appeared at about 815 nm and the colour changed from green to blue since the valley of the spectrum shifted to left about 50 nm. Optical band gap values were elucidated from the onset of the neutral optical bands of the polymers and determined as 1.81 eV for P**CBT** and 1.44 for P**CTBTC** (1.70 eV for P**TBT** [38]).

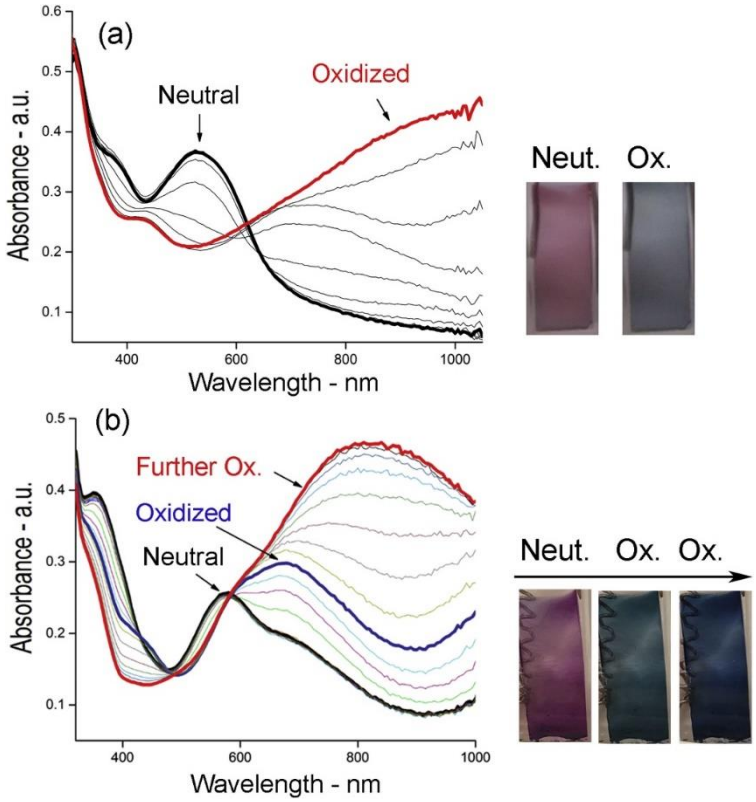

Figure 3.8. UV-Vis Spectra and photos of the films of a) P**CBT** and b) P**CTBTC** during oxidation (scan rate 20 mV/s)

Kinetic study was performed on P**CBT** and P**CTBTC** to reveal the percent transmittance (T%) values and the switching times. As it is noted before, electrochemical stability of the polymers was found to be not promising. For this

reason, constant potentials required for oxidation and reduction were applied with 10 s intervals to elucidate basic kinetic data. The percent transmittance was measured as 12% for P**CBT** (at 530 nm) and the switching time was calculated as 3 s at 95% of the full contrast which are similar to the values given for P**TBT** (percent transmittance of 15% and switching time of 3 s) [38]. For P**CTBTC**, on the other hand, T% and the switching time were found as 8% and 4.2 s, respectively (at 576 nm). The properties of the polymer films are summarized in Table 3.3.

Table 3.3. Optical and electrochemical properties of polymer films

Polymers	λ_{max} (nm)		E^{ox}_{onset}(V)	E_g^{opt} (eV)	Color in neutral state	Color in oxidized state	T %	$T_{switching}$ (s)
P**TBT** [38]	373	554	0.71	1.70	Magenta	Cyan	15	3
P**CBT**	373	530	0.80	1.81	Pale Pink	Greenish Blue	12	3
P**CTBTC**	353	576	0.65	1.44	Pinky	Green/Blue	8	4.2
P**TCBCT** [39]	365	450	0.95	-	-	-	-	-

CHAPTER 4

CONCLUSIONS

A series of DAD and DAD' type monomers and their polymers were synthesized utilizing 2,1,3-benzothiadiazole (**B**) as the acceptor unit and 9-benzyl-9H-carbazol (**C**) and thiophene (**T**) as the donor units. The electrochemical and optical properties of the newly synthesized monomers and polymers were investigated to elucidate the effect of different donor units. Electrochemical and optical properties of **C** and **T** containing unsymmetrical monomer, **CBT**, was found to be between that of symmetrical **CBC** and **TBT** monomers (i.e E^{ox}_{onset}(**CBC**)< E^{ox}_{onset}(**CBT**)< E^{ox}_{onset}(**TBT**) and λ_{max}(**CBC**)< λ_{max} (**CBT**)< λ_{max} (**TBT**)). The red shift observed in the lower energy absorption band of monomers with successive replacement of **C**-donor unit with **T**-donor unit was explained in terms of increasing ICT between D and A units. Solvatochromic behavior of the monomers were also studied in solvents of different polarities and the emission spectra results indicate that the observed positive solvatochromism of the monomers present ICT-type fluorophores that are highly polarized in their excited states. D−A−D′ asymmetric structure, which causes a change in the electron cloud distribution and as a result, the number of metastastable states, and redox-active states increases, compared with those of the symmetrically structured monomer. Combining both **C** and **T** units symmetrically in the same structure (**CTBTC**), on the other hand, exhibited the lowest oxidation potential and greatest red shift among the others due to increased π-conjugation and ICT, respectively.

Although electrochemical polymerization of **CBC** was unsuccessful, **CBT** and **CTBTC** were successfully polymerized to their corresponding polymer films, P**CBT** and P**CTBTC** both on Pt-disc and ITO working electrodes. Electrochemical and optical properties of polymer films were also investigated and compared with that of previously reported P**TBT**. It was found that P**CTBTC** exhibited the lowest

E_g value. Albeit its multichromic behavior during oxidation, P**CTBTC** was found have lower electrochemical stability (loss of 38 % of its electroactivity after 10 cycles) and longer switching time (t_s= 4.2 s) as compared to P**CBT** and P**TBT**. These results show that P**CBT** can be the most proper candidate that can be used in optoelectronic applications like electrochromic devices due to its better stability and faster response. The introduction of different donor groups on both sides of the same acceptor unit (P**CBT**) changes the optical and electrochemical properties of the polymer. Bridging thiophene units in D-A-D type structure (P**CTBTC**) results in multichromic behaviour during oxidation and lowest E_g value.

REFERENCES

[1] Shrikawa, H., Louis, E. J., MacDiarmid, A. G., Chiang, C. K., & Heeger, A. J. (1977). Synthesis of Electrically Conducting Organic Polymers : Halogen Derivatives of Polyacetylene, (CH),. *J.C.S. Chem. Comm.*, 578-580.

[2] Reynolds, J. R. (2014). Pi-Conjugated Polymers: The Importance of Polymer Synthesis. In K. Müllen, J. R. Reynolds, & T. Masuda, *Conjugated Polymers: A Practical Guide to Synthesis* (pp. 1-11). The Royal Society of Chemistry.

[3] Epstein, A. J. (1999). Electrical Conductivity in Conjugated Polymers. In L. Rupprecht, *Conductive Polymers and Plastics in Industrial Applications* (pp. 1-9). William Andrew Publishing.

[4] Mortimer, R. J., Rosseinsky, D. R., & Monk, P. M. (2015). *Electrochromic Materials and Devices.* Weinheim: Wiley-VCH Verlag GmbH & Co.

[5] Kim, Y., Han, M., Kim, J., & Kim, E. (2018). Electrochromic capacitive windows based on all conjugated polymers for a dual function smart window. *Energy Environ. Sci.*, 2124-2133.

[6] Wang, P.-C., Liu, L.-H., Mengistie, D. A.-H., Wen, B.-J., Liu, T.-S., & Chu, C.-W. (2013). Transparent electrodes based on conducting polymers for display. *Displays*, 301-314.

[7] Kraft, A., Grimsdale, A. C., & Holmes, A. B. (1998). Electroluminescent Conjugated Polymers-Seeing Polymers in a New Light. *Angew. Chem. Int. Ed*, 402-428.

[8] Sariciftci, N. S., Smilowitz, L., Heeger, A. J., & Wudi, F. (1992). Photoinduced Electron Transfer from a Conducting Polymer to Buckminsterfullerene. *Science*, 1474-1476.

[9] Borole, D. D., Kapadi, U. R., Mahulikar, P. P., & Hundiwale, D. G. (2006). Conducting polymers: an emerging field of biosensors. *Des. Monomers Polym.*, 1-11.

[10] Chandrasekhar, P., Zay, B. J., McQueeney, T., Scara, A., Ross, D., Birur, G. C., Douglas, D. (2002). Conducting Polymer (CP) infrared electrochromics in spacecraft thermal control and military applications. *Synth. Met*, 23-24.

[11] Alshammary, B., Walsh, F. C., Herrasti, P., & Ponce de Leon, C. (2016). Electrodeposited conductive polymers for controlled drug release: polypyrrole. *J Solid State Electrochem*, 839-859.

[12] Anguera, G., & Sanchez-Garcia, D. (2014). Conjugated polymers: Synthesis and applications in optoelectronics. *AFINIDAD LXXI*, 251-262.

[13] Eken, S., Cansu Ergun, E. G., & Önal, A. M. (2016). Synthesis and Electrochemical Polymerization of Dithienosilole-Based Monomers Bearing Different Donor Units. *J. Electrochem. Soc.*, G69-G74.

[14] Bakhshi, A. K., Kaur, A., & Arora, V. (2012). Molecular engineering of novel low band gap conducting polymers. *Indian J. Chem.*, 57-68.

[15] Li, W., & You, W. (2014). Donor–Acceptor Alternating Copolymers. In K. Müllen, J. R. Reynolds, & T. Masuda, *Conjugated Polymers: A Practical Guide to Synthesis* (pp. 319-342). The Royal Society of Chemistry.

[16] Rasmussen, S. (2013). Low-Bandgap Polymers. In S. Kobayashi, & K. Müllen, *Encyclopedia of Polymeric Nanomaterials* (pp. 1-13). Berlin: Springer.

[17] Chen, M., Perzon, E., Andersson, M. R., Marcinkevicius, S., Jönsson, S. K., Fahlman, M., & Berggren, M. (2004). 1 micron wavelength photo- and

electroluminescence from a conjugated polymer. *Appl. Phys. Lett.*, 3570-3572.

[18] Bundgaard, E., & Krebs, F. C. (2007). Low band gap polymers for organic photovoltaics. *Sol. Energy Mater. Sol. Cells*, 954-985.

[19] Havinga, E. E., Hoeve, W. T., & Wynberg, H. (1992). A new class of small band gap organic polymer conductors. *Polym. Bull.*, 119-126.

[20] Peng, H., Sun, X., Weng, W., & Fang, X. (2017). Synthesis and Design of Conjugated Polymers for Organic Electronics. In *Polymer Materials for Energy and Electronic Applications* (pp. 9-61). Amsterdam: Academic Press.

[21] Solomons, T. G., Fryhle, C. B., & Snyder, S. A. (2014). *Organic Chemistry.* United States of America: Wiley.

[22] Otero, T. F. (2016). Electrochemical Methods. In *Conducting Polymers: Bioinspired Intelligent Materials and Devices* (pp. 12-25). The Royal Society of Chemistry.

[23] Azman, N. H., Lim, H. N., & Sulaiman, Y. (2015). Effect of electropolymerization potential on the preparation of PEDOT/graphene oxide hybrid material for supercapacitor application. *Electrochim. Acta*, 785-792.

[24] Ponder, J. F., & Reynolds, J. R. (2017). Conducting Polymers : Redox States in Conjugated Systems. In E. Da Como, & v. H. Elizabeth, *The WSPC Reference on Organic Electronics: Organic Semiconductors.* World Scientific.

[25] Otero, T. F. (2016). Electrosynthesis of Conducting Polymers. In *Conducting Polymers: Bioinspired Intelligent Materials and Devices* (pp. 26-58). The Royal Society of Chemistry.

[26] Kraft, A. (2018). Electrochromism: a fascinating branch of electrochemistry. *ChemTexts*, 1-18.

[27] Mortimer, R. J. (2011). Electrochromic Materials. *Annu. Rev. Mater. Res.*, 241-268.

[28] Cansu-Ergun, E. G., & Önal, A. M. (2018). Carbazole based electrochromic polymers bearing ethylenedioxy and propylenedioxy scaffolds. *J. Electroanal. Chem.*, 158-165.

[29] Karpicz, R., Puzinas, S., Krotkus, S., Kazlauskas, K., Jursenas, S., Grazulevicius, J. V., Gulbinas, V. (2011). Impact of intramolecular twisting and exciton migration on emission efficiency of multifunctional fluorene-benzothiadiazole-carbazole compounds. *J. Chem. Phys.*, 204508-(1-8).

[30] Akbayrak, M., & Önal, A. M. (2016). Synthesis and electrochemical polymerization of diketopyrrolopyrrole based donor–acceptor–donor monomers containing 3,6- and 2,7-linked carbazoles. *Polym. Chem.* , 6110-6119.

[31] Wang, Y., & Michinobu, T. (2016). Benzothiadiazole and its p-extended, heteroannulated derivatives: useful acceptor building blocks for high-performance donor– acceptor polymers in organic electronics. *J. Mater. Chem. C*, 6200-6214.

[32] Çakal, D., Boztaş, Y., Akdag, A., & Önal, A. M. (2019). Investigation of Fluorine Atom Effect on Benzothiadiazole Acceptor Unit in Donor Acceptor Donor Systems. *J. Electrochem. Soc.*, G141-G147.

[33] Liu, J., Li, L., Xu, R., Zhang, K., Ouyang, M., Li, W., Zhang, C. (2019). Design, Synthesis, and Properties of Donor−Acceptor−Donor′ Asymmetric Structured Electrochromic Polymers Based on Fluorenone as Acceptor Units. *ASC Appl. Polym. Mater.* , 1081-1087.

[34] Geng, J., Dai, Y., Wang, X.-X., Hu, M.-Y., Tao, T., & Huang, W. (2015). Substitution effects on the properties of 10,13-disubstituted dipyrido[3,2-a:2′,3′-c]phenazine donor–acceptor compounds and their ruthenium(II) complexes. *Tetrahedron*, 654-662.

[35] Castro, E., Cabrera-Espinoza, A., Deemer, E., & Echegoyen, L. (2015). Low-Energy-Gap Organic Based Acceptor–Donor–Acceptor π-Conjugated Small Molecules for Bulk-Heterojunction Organic Solar Cells. *Eur. J. Org. Chem*, 4629-4634.

[36] Zhu, H., Li, M., Hu, J., Wang, X., Jie, J., & Guo, Q. (2016). Ultrafast Investigation of Intramolecular Charge Transfer and Solvation Dynamics of Tetrahydro[5]-helicene-Based Imide Derivatives. *Sci. Rep.*, 1-12.

[37] Yasutani, Y., Honsho, Y., Saeki, A., & Seki, S. (2012). Polycarbazoles: Relationship between intra- and intermolecular charge carrier transports. *Synth. Met.* , 1713-1721.

[38] Cansu-Ergun, E. G., Akbayrak, M., Akdag, A., & Önal, A. M. (2016). Effect of Thiophene Units on the Properties of Donor Acceptor Type Monomers and Polymers Bearing Thiophene-Benzothiadiazole- Scaffolds. *J. Electrochem. Soc.*, G153-G158.

[39] Ding, G., Lin, T., Zhou, R., Dong, Y., Xu, J., & Lu, X. (2014). Electrofluorochromic Detection of Cyanide Anions Using a Nanoporous Polymer Electrode and the Detection Mechanism. *Chem. Eur. J.*, 13226 – 13233.

APPENDICES

A. NMR Data

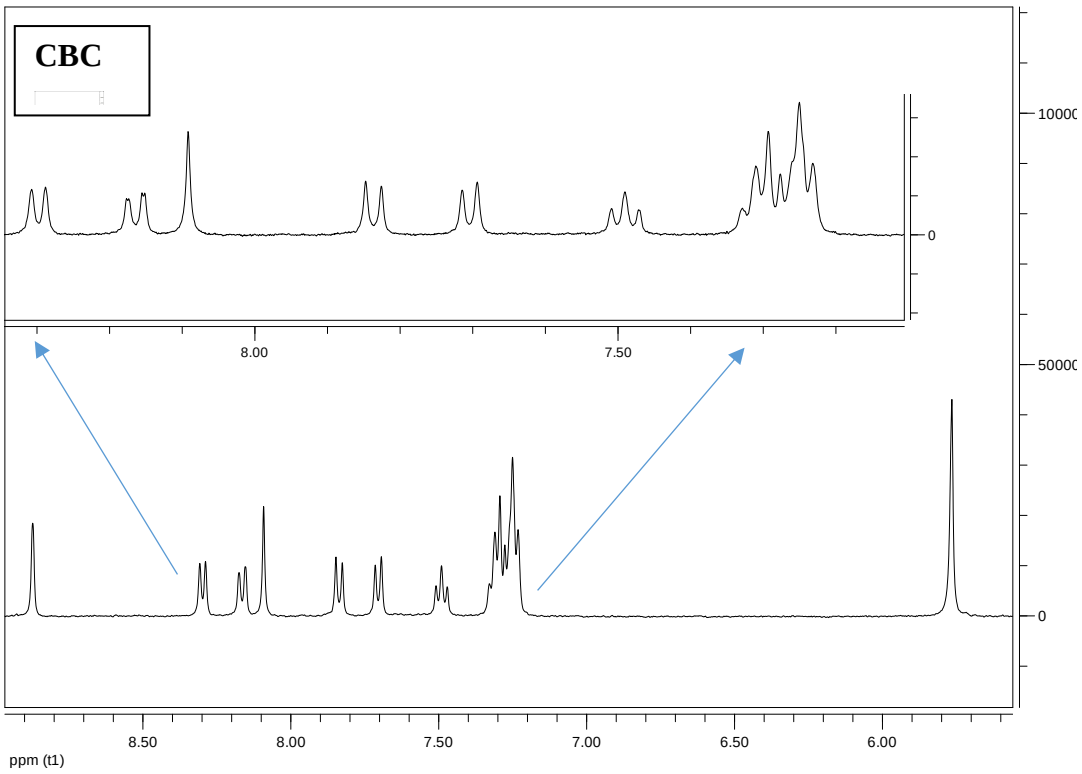

Figure A.1. ^{1}H NMR of CBC monomer

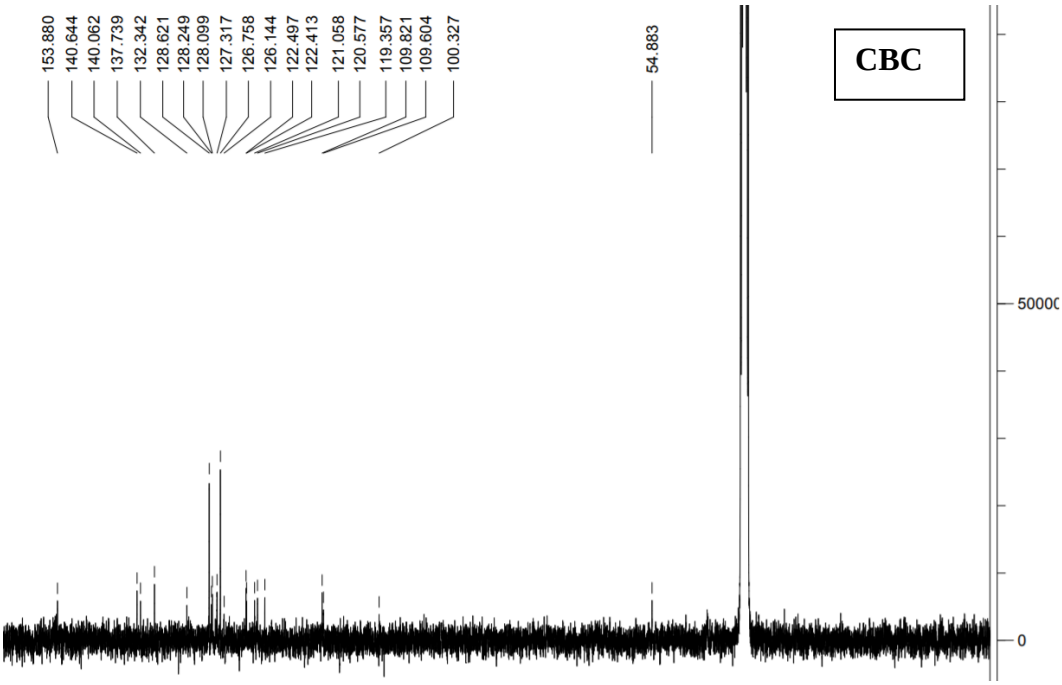

Figure A.2. ^{13}C NMR of CBC monomer.

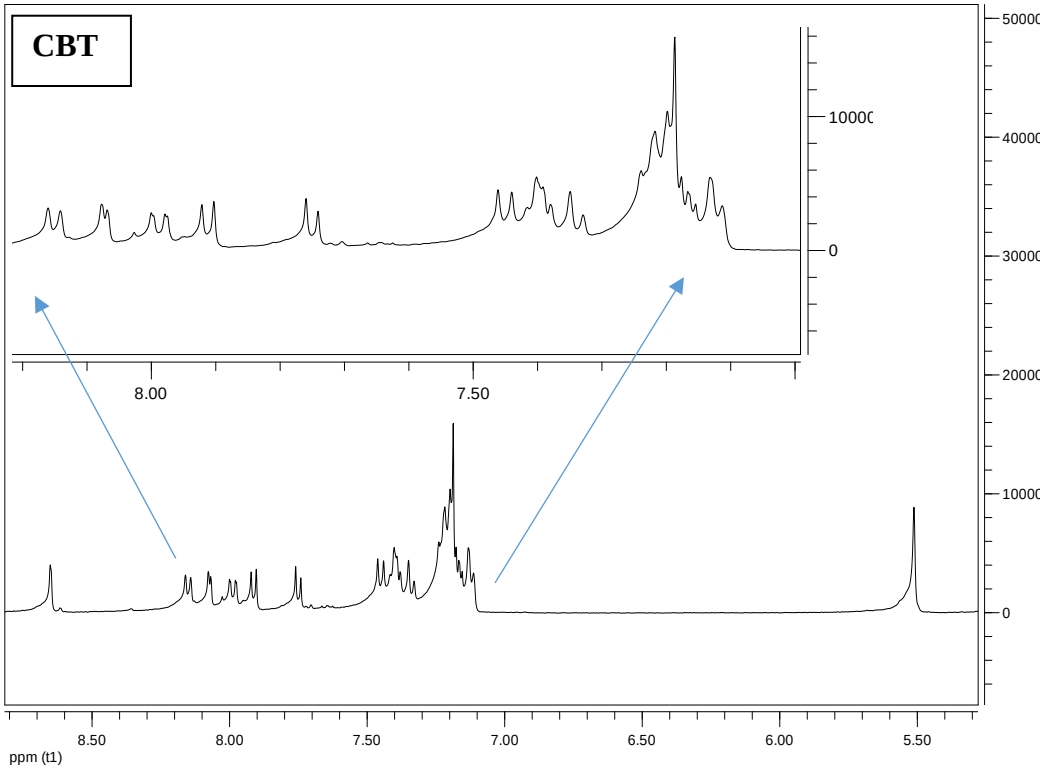

Figure A.3. ^{1}H NMR of CBT monomer

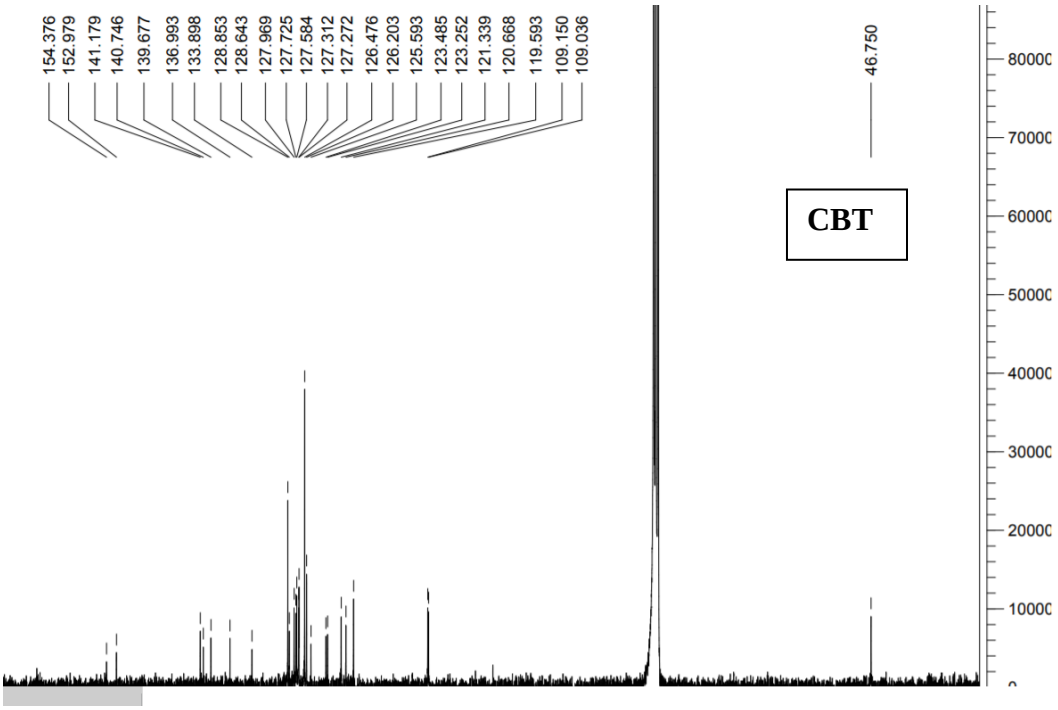

Figure A.4. ^{13}C NMR of CBT monomer

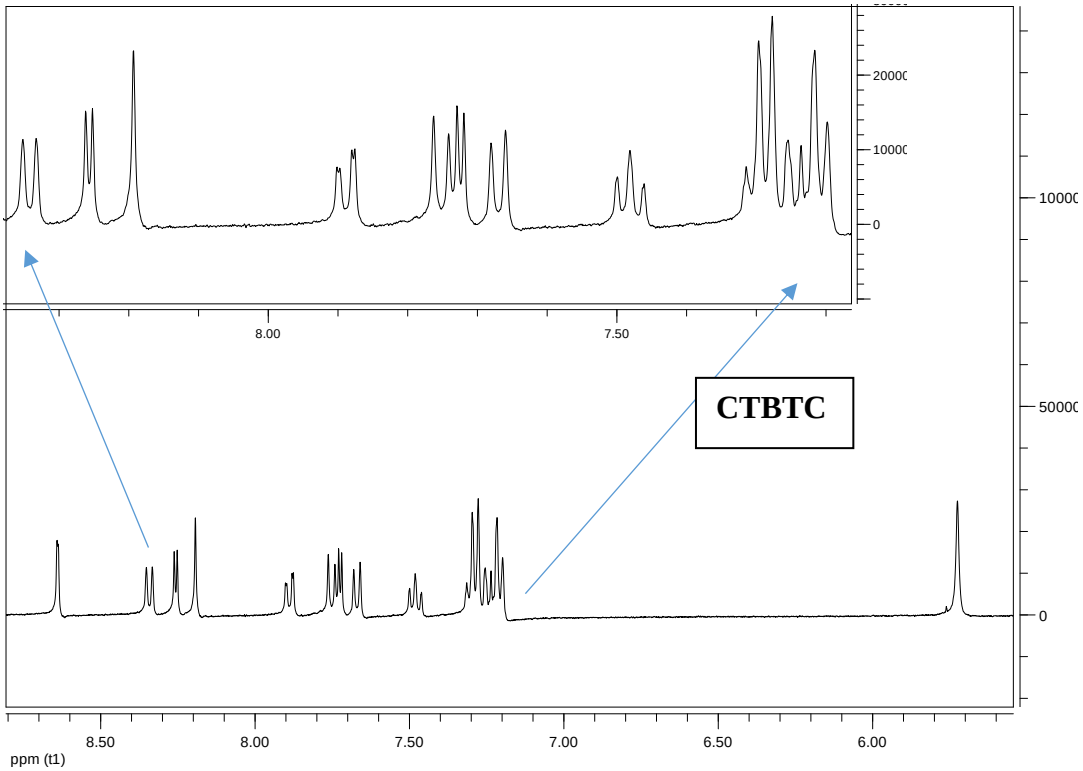

Figure A.5. ^{1}H NMR CTBTC monomer

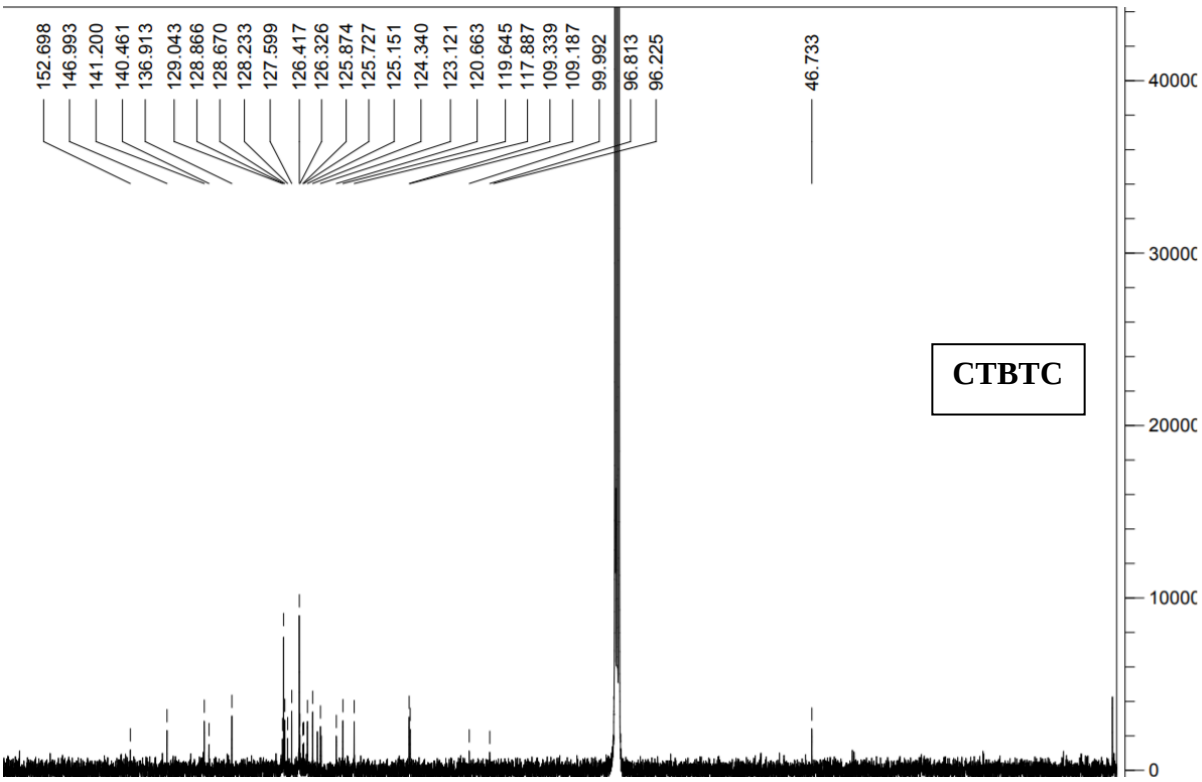

Figure A. 6. ^{13}C NMR of CTBTC monomer